Journal of Innovative Materials in Extreme Conditions
2023
Volume 4
Issue 2

A REVIEW OF THE SYNTHESIS OF COMPOSITIONALLY COMPLEX ULTRA-HIGH-TEMPERATURE CERAMICS

Dharma Teja Teppala[1,]*, Samuel Aeneas Kredel[1], Emanuel Ionescu [1,2], Branko Matović[3]

[1]TU Darmstadt, Institute for Material Science, Otto-Berndt-Str. 3, D-64287, Darmstadt, Germany
[2]Fraunhofer IWKS, Brentanostr. 2a, D-63755 Alzenau, Germany
[3]Center for Synthesis, Processing, and Characterization of Materials for Application in the Extreme Conditions-CextremeLab, Institute of Nuclear Sciences Vinča, Belgrade, Serbia
Corresponding author: dharma.teppala@stud.tu-darmstadt.de*

Abstract: *Ultra-high temperature ceramics (UHTC) are a class of ceramics that possess melting points greater than 3000 °C and can withstand temperatures higher than 2000 °C without structural failure. The need to increase the performance inherently leads to the implementation of extreme temperatures, leading to the search for a new class of materials with better thermal properties. Compositionally complex ultra-high temperature ceramics with the inclusion of additional elements, whether resulting in an equimolar or non-equimolar site occupation in the respective sublattices, can improve properties due to the contributions of the configurational entropy. The term compositional complexity can be used as an umbrella term for the class of compositions with 3 or more elements and also their non-equimolar parts. The current review paper is based on the classification of the different compositionally complex ultrahigh temperature ceramics as borides, carbides, nitrides, etc., and reviews the different procedures employed for the bulk or powder synthesis thereof.*

Keywords**:** *UHTC, Compositional Complexity, Carbides, Nitrides, Borides, Silicides*

1. Introduction

Ultra-high-temperature ceramics (UHTC) are materials that have melting points greater than 3000 °C and may provide structural stability during operation at temperatures up to 2000 °C [58]. These ceramics are mainly based on the non-oxides of the transitional metal from group IV (Ti, Zr, Hf), and V (V, Nb Ta), among those being (di)borides, carbides, nitrides, or silicides. The high-temperature stability of these compounds is mainly due to the covalent bonds between B, C, and N with any of the group IV, and V elements. The presence of covalent bonds is the reason for high melting points, outstanding mechanical properties, and oxidation resistance. Additionally, UHTCs possess better electrical and thermal properties than oxides due to their metallic character [58].
Compositionally complex ceramics is the coinage for the group of ceramics that consist of medium, high entropy ceramics along with non-equimolar quaternary ceramics. Although the high entropy concept was introduced initially with the alloys, the use of the high entropy concept accelerated the ceramic property development. The compositional complexity is based on the Gibbs energy and the Boltzmann formula of entropy.

$$\Delta G_{mix} = \Delta H_{mix} - T\Delta S_{mix} \quad (1)$$

$$S = k_B \ln \omega \quad (2)$$

ΔG_{mix}: Gibbs free energy of mixing, ΔH_{mix}: Enthalpy of mixing, ΔS_{mix}: configurational entropy, S: entropy, k_b: Boltzmann constant, ω: number of possible configurations.
At sufficiently high temperatures, the $T\Delta S_{mix}$ term in eq. (1), with the entropy S being given by eq. (2), dominates the Gibbs energy and thus significantly contributes to a thermodynamic stabilization of the phase.

Along with the entropy, many other parameters such as VEC (Valance Electron Concentration), mixing enthalpy, and rules similar to Hume-Rothery were introduced and considered to be highly correlated to the thermodynamic stability of single-phase compositionally complex ceramics. Although the above-mentioned criteria are not definite for the formation of the high entropy material, a trend for the formation of a high entropic phase can be expected. In the case of the ceramics, additional contribution from the anionic sublattice can be expected, leading to the increase of the mixing entropy.

Substitution of the multiple transitional elements in the cationic sublattice of compositionally complex UHTCs can result in lattice distortions resulting in the hindrance of phonon propagation and increased electron scattering resulting in lower thermal and electrical conductivities over the binary UHTC themselves. The case can also be justified with substitution with an anionic sublattice or both.

The UHTC is generally used in aerospace applications involving high temperatures, resulting in their need for powder, bulk, and coatings. Traditional techniques for densification such as spark plasma sintering (SPS) and hot pressing are used. Additionally, non-traditional methods such as molten-salt-assisted methods were also employed to obtain compositionally complex powders, especially in the case of borides and carbides.

The current review paper will focus on the various compositionally complex borides, carbides, (carbo)nitrides, silicides, etc. of transitional metals of groups IV, V, and VI, summarizing the various procedures employed for their synthesis.

2. Brief consideration of compositional complexity in ceramics

In a multi-element compositional space for an alloy considering the various possible combinations, the compositions corresponding to the center region of the phase diagrams are generally considered as high entropy materials, with a preset of at least 5 or more elements, as the mixing entropy would be sufficiently large enough to overcome the effects of enthalpy. The entropy of mixing ΔS_{mix} can be derived using Stirling's approximation, eq. (3). Assuming anionic and cationic sublattice contributions, eq. (4) can be obtained.

$$\Delta S_{mix} = -R * \sum_{i=1}^{n} x_i \ln x_i \quad (3)$$

$$\Delta S_{mix} = -R\left(\sum_{i=1}^{n} c_i \ln c_i + \sum_{j=1}^{m} a_j \ln a_j\right) \quad (4)$$

R: Ideal gas constant, *x*: mole fraction, *c*: cationic site occupancy, *a*: anionic site occupancy.
In the case of the medium entropy, the number of elements is between 3 and 5 (see Figure 1).

Due to the entropic part of the Gibbs energy being able to overcome the enthalpy, a single-phase solid solution may be favored against the other possible outcomes. As the number of elements increase, due to difference in size, and chemical properties, many unexpected properties can be seen.

Based on the concept of high and medium entropy, compositionally complex ceramics are developed, where (a) the mixing entropy has a contribution from either the cationic and the anionic site (b) the number of elements inclusive of the cationic and anionic sublattices can be greater than or equal to 5.

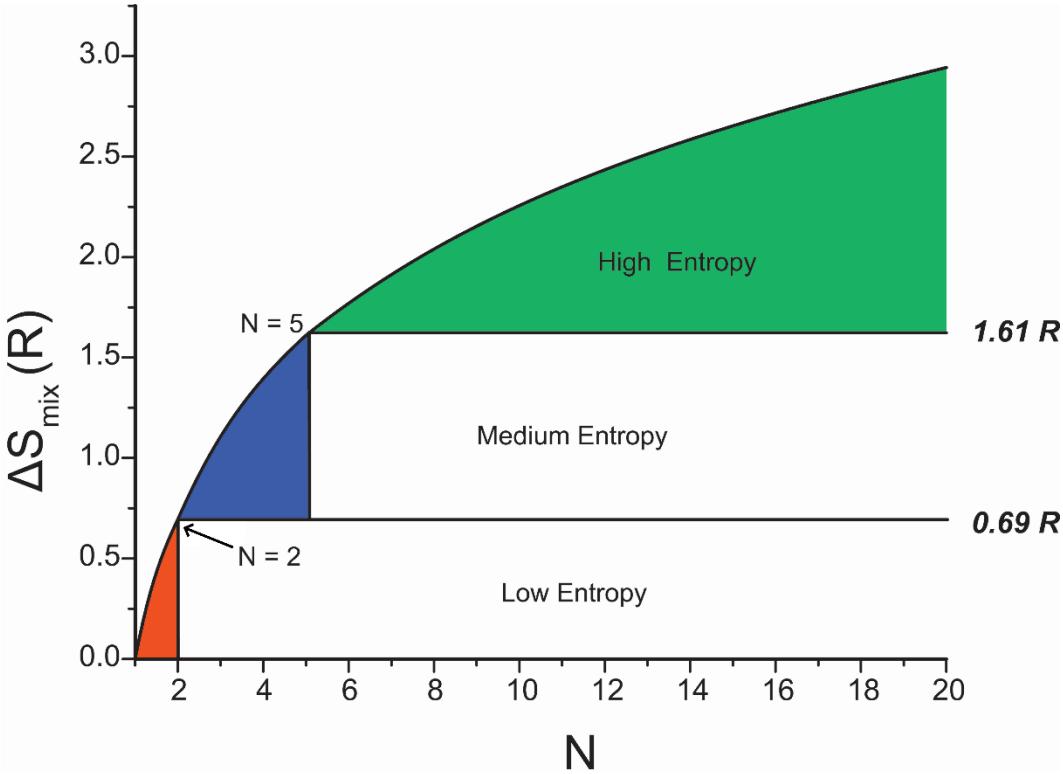

Figure 1. Configurational entropy vs number of elements in case of alloys.

Although a lot of element combinations are possible, other parameters such as the deviation parameter δ, given by eq. (5), corresponding to atomic lattice parameter mismatch were also introduced. In the case of the ceramics, it was stated that δ should have a deviation of less than 4% in order to obtain a single phase; however, various compositions with δ being greater than 4% were also observed as single-phase materials.

$$\delta = \sqrt{\sum_{i=1}^{n} c_i \left(1 - \frac{a_i}{\bar{a}}\right)^2} \qquad (5)$$

δ: deviation parameter, a: lattice constant, $\bar{a}$: mean lattice parameter, c: concentration.

To avoid the discrepancy, Gild et.al [77] suggested considering the lattice parameter instead of atomic size to better represent the single-phase formability. In the case of boride systems, the change in the c direction was observed to be more useful in predicting single-phase formability [77].

Other properties such as entropy forming ability (EFA) were computed theoretically by Sarker et.al [30] and were also considered during the design of high-entropy ceramics, EFA being a measure of the likelihood of a material system to form a single phase, obtained by observing possible unit cell configurations and evaluating their energies.

Although the high-entropy ceramics are observed and found to be promising materials, the non-equimolar combinations and ternary compositions of the high entropy compositional space were also found to exhibit similar to or better mechanical and thermal properties, thus the term compositionally complex ceramics has come into existence by grouping up the medium, non-equimolar and high entropy ceramics.

3. Synthesis Methods for Ultra-High Temperature Compositionally Complex Ceramics

As these materials need to withstand application temperatures higher than 2000 °C, a prerequisite of the present phases is a substantially high melting point (i.e., beyond 3000 °C), making high temperatures necessary to yield dense and structurally rigid materials. Thus, the fabrication of the ceramics seems difficult. Many methods are currently being employed for the synthesis to overcome these complications, and these can be majorly classified as solid-state synthesis [7],[18],[24],[26],[29],[40],[59],[60],[69].

Thus, various classes of UHTCs (see Figure 2) were preparatively accessed by using synthesis methods such as carbo- and borothermal reduction [3], [65], [85], [90], [91], reactive sintering of the elements [2], [7], [8], [16], [43], [50], [70], [72], [74], [75], [77], [87], molten salt synthesis [61], [64], [88], [89], sol-gel synthesis [29], [31], [63], [69], [96], arc melting [62], [92], [93] and high pressure [19], [94], [97]. The processing can also involve multiple steps consisting of combinations of these methods to favor the random distribution of constituents in cationic and anionic sublattices.

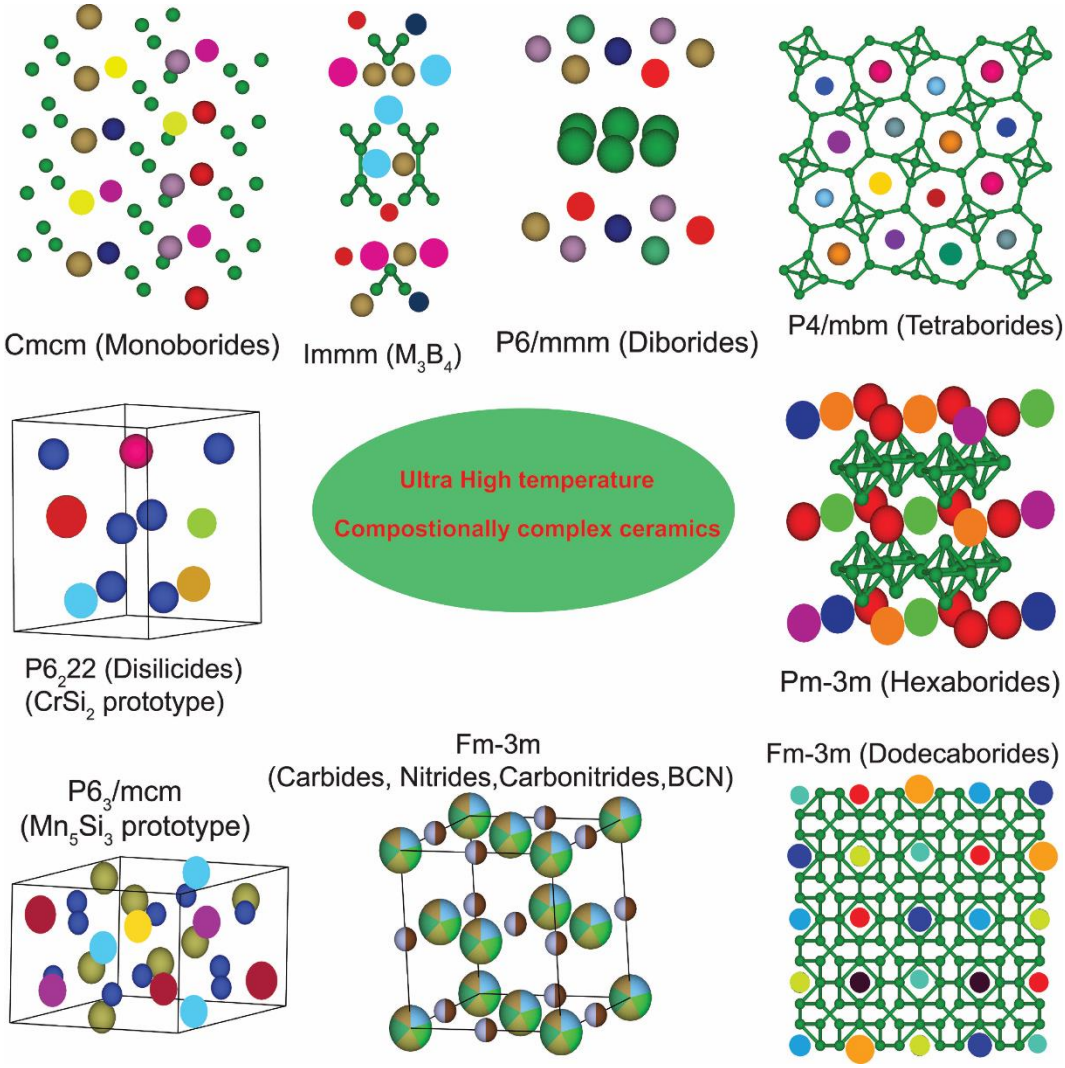

Figure 2. Various classes of compositionally complex UHTCs synthesized so far and their experimentally observed crystalline structures.

3.1 Solid State Synthesis

Solid state synthesis is a straightforward reaction, suitable for solid reactants. This process involves the reaction of the individual constituents. Tallarita et al. [7] have synthesized $(Hf_{0.2}Mo_{0.2}Ta_{0.2}Nb_{0.2}Ti_{0.2})B_2$ by reacting a ball-milled mixture of Hf, Mo, Ta, Nb, and Ti metal powders along with boron to obtain a high entropy diboride, according to the following eq. (6).

$$0.2Hf + 0.2Mo + 0.2Ta + 0.2Nb + 0.2Ti + (2 + x)B = (Hf_{0.2}Mo_{0.2}Ta_{0.2}Nb_{0.2}Ti_{0.2})B_2 \quad (6)$$

The self-propagated reaction of the mixture occurred with W filament as the heating source. Excess boron was used to reduce the oxide impurities. However, a small contribution of additional phases such as HfO_2, (Hf, Ti)B_2, (Ti, Ta)B_2, and HfB_2 were found through XRD investigations.

Recently Zhao et. al [59], [60] synthesized $(V_{0.2}Mo_{0.2}W_{0.2}Nb_{0.2}Ni_{0.2})B$, $(V_{0.2}Cr_{0.2}Mo_{0.2}Ni_{0.2}W_{0.2})B$, $(V_{0.2}Mo_{0.2}Ta_{0.2}Ni_{0.2}W_{0.2})B$, $(V_{0.2}Cr_{0.2}Mo_{0.2}W_{0.2}Ti_{0.2})B$ and $(Cr_{0.2}Mo_{0.2}Ta_{0.2}Ni_{0.2}W_{0.2})B$ via reactive hot pressing of ball milled mixtures of the compositions mentioned above. Although there were oxide and diboride phases, the sintering of these compositions at 2000 °C resulted in high entropic monoborides except for $(V_{0.2}Cr_{0.2}Mo_{0.2}W_{0.2}Ti_{0.2})B$ as significant TiB_2 was observed even at 2000 °C. However, Ye et al. [65] used ball mill-assisted hot pressing for $(Ti_{0.333}Zr_{0.333}Hf_{0.333})B_2$ at 1900 °C.

Chicardi et al. [26], [40] used a simple mechanochemical method for $(Ti_{0.2}Zr_{0.2}Hf_{0.2}V_{0.2}Nb_{0.2})C$, $(Ti_{0.2}Zr_{0.2}Hf_{0.2}V_{0.2}Ta_{0.2})C$, $(Ti_{0.2}Zr_{0.2}Hf_{0.2}Nb_{0.2}Ta_{0.2})C$, $(Ti_{0.2}Zr_{0.2}V_{0.2}Nb_{0.2}Ta_{0.2})C$, $(Ti_{0.2}Hf_{0.2}V_{0.2}Nb_{0.2}Ta_{0.2})C$ and $(Zr_{0.2}Hf_{0.2}V_{0.2}Nb_{0.2}Ta_{0.2})C$, via a long duration (/extended) ball milling at room temperature. In the case of $(Ti_{0.2}Zr_{0.2}V_{0.2}Nb_{0.2}Ta_{0.2})C$, the metallic powders were mixed with carbon and ball milled for 70 h under 5 atm of Ar, with an interval of 5 h of ball milling and 1 h of pause to avoid a temperature increment, thereby obtaining the high entropy carbide without any involvement of heating.

In the case of nitrides, Jin et al. [29] synthesized $(V_{0.2}Nb_{0.2}Cr_{0.2}Mo_{0.2}Zr_{0.2})N$ by reacting chlorides of V, Cr, Nb, Mo, and Zr with urea. The chlorides were reacted with urea under the mechanical influences of ball milling for 30 min which resulted in gelation. The gel was later pyrolyzed at 800 °C under N_2 resulting in $(V_{0.2}Nb_{0.2}Cr_{0.2}Mo_{0.2}Zr_{0.2})N$.

Similar steps were followed for $(Hf_{0.2}Nb_{0.2}Ta_{0.2}Ti_{0.2}V_{0.2})N$ by Xing et. al,[69] however ethanol was used during milling and the pyrolysis temperature was 1300 °C.

However, Guan et al. [18] have applied this method to obtain borocarbonitrides with a simple two-step mechanical alloying. $(Ta_{0.2}Nb_{0.2}Zr_{0.2}Hf_{0.2}W_{0.2})BCN$, $(Ta_{0.2}Nb_{0.2}Zr_{0.2}Hf_{0.2}Ti_{0.2})BCN$, and $(Ta_{0.2}Nb_{0.2}Zr_{0.2}Ti_{0.2}W_{0.2})BCN$ were synthesized by mechanical alloying of amorphous BCN with the respective metallic powders. The amorphous BCN was prepared by 10 h of milling of h-BN and graphite. The respective metallic powders were added in the second step of mechanical alloying, which continued for 24 hours.

Zhao et al. [24] have involved Al to obtain $(Ti_{0.25}V_{0.25}Nb_{0.25}Ta_{0.25})C$. The elements were mixed in a composition similar to 20 at% of HEC and 80 at% Al. The respective powders were ball milled using ZrO_2 and were calcinated at different temperatures leading to a high entropy carbide in the Al matrix. The aluminum formed intermetallics at low temperatures, but when pyrolyzed at high temperatures, it resulted in a single-phase carbide because Al was acting as a solvent, facilitating diffusion (see Figure 3).

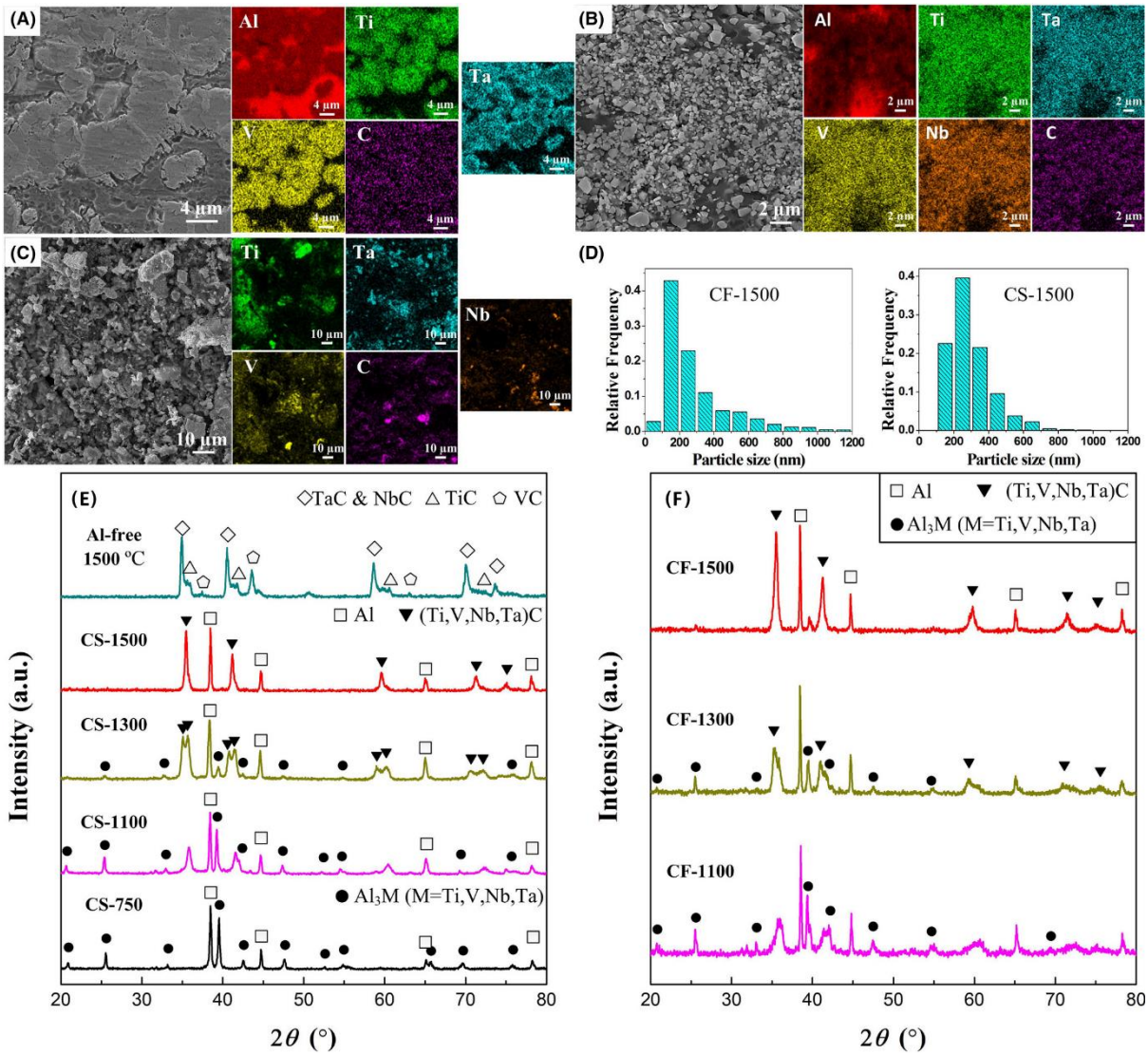

Figure 3. (A)-(C) SEM images of (TiTaNbV)C alloyed with Al, (TiTaVNb)C alloyed with Al and (TiTaVNb)C without Al. (E)-(F) displays the XRD of the compositions obtained at different temperatures and clearly shows the effect of Al on obtaining a single phase. Reprinted from Zhao et. al. [24]

3.2 Carbo-/ Borothermal Reductions

These methods are usually employed when the preparative access to the UHTCs is anticipated from oxidic precursors. A thorough mixing or milling of the respective oxides along with a reactant source forms the compositionally complex ceramic.

Zhang et al. [3] prepared $(Hf_{0.2}Zr_{0.2}Ta_{0.2}Nb_{0.2}Ti_{0.2})B_2$, $(Hf_{0.2}Zr_{0.2}Mo_{0.2}Nb_{0.2}Ti_{0.2})B_2$ and $(Hf_{0.2}Mo_{0.2}Ta_{0.2}Nb_{0.2}Ti_{0.2})B_2$ $(Hf_{0.2}Zr_{0.2}Ta_{0.2}Cr_{0.2}Ti_{0.2})B_2$ – hexagonal diboride compositions. The appropriate amounts of the oxides for the target compositions were thoroughly roll-milled (for 24 h with Si_3N_4 milling balls along with B_4C, acting as a source for both carbon and boron. The compositions were heated under vacuum at 1600 °C resulting in compositionally complex diborides and small amounts of polymorphs of HfO_2.

Zhang et al. [91] synthesized a quaternary diboride, $(Hf_{0.25}Zr_{0.25}Ta_{0.25}Sc_{0.25})B_2$, by ball milling the respective oxides and B_4C in ethanol, with zirconia as milling balls, then pressing cylindrical pellets to ensure contact during pyrolysis at 1700 °C under vacuum for 2 h, leading to the formation of a single phase compositionally complex ceramic.

Cui et. al [100] synthesized the first high-entropy dodecaboride $(Dy_{0.2}Ho_{0.2}Er_{0.2}Tm_{0.2}Lu_{0.2})B_{12}$ and subsequently $(Dy_{0.166}Ho_{0.166}Er_{0.166}Tm_{0.166}Lu_{0.166}Hf_x)B_{12}$ by reacting Dy_2O_3, Ho_2O_3, Er_2O_3, Tm_2O_3 and Lu_2O_3 with excess boron (see Figure 4). In the case of the latter composition, HfO_2 was included in the reaction. The powders were thoroughly ground in a pot for 24 h with ethanol and ZrO_2 balls, then pressed as cylindrical pellets and subsequently pyrolyzed in a vacuum at 1600 °C for 1 h. The obtained powders were either densified by spark plasma sintering (SPS) with a pressure of 30 MPa at 1500 °C, 1600 °C, 1700 °C, and 1800 °C for 5 min or high-pressure sintering at 5 GPa at 1700 °C for 30 min. This exact synthesis procedure was also followed for the hexanary composition.

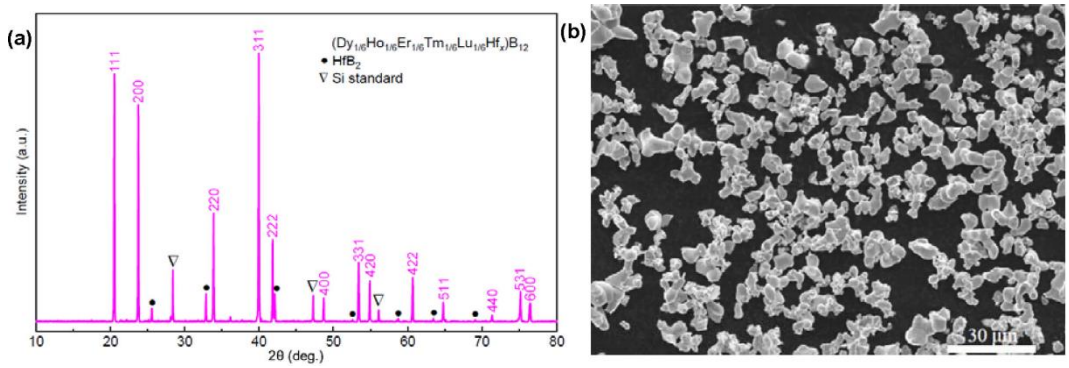

Figure 4. (a) XRD of the dodecaboride with HfB_2 impurity. (b) SEM image of the obtained powders. Reprinted with permission from Cui et al. [100]

The EDS mappings and TEM characterization were performed and the particles were segregated as Hf-rich, rare earth-rich, and B-rich, layered, phases (see Figure 5).

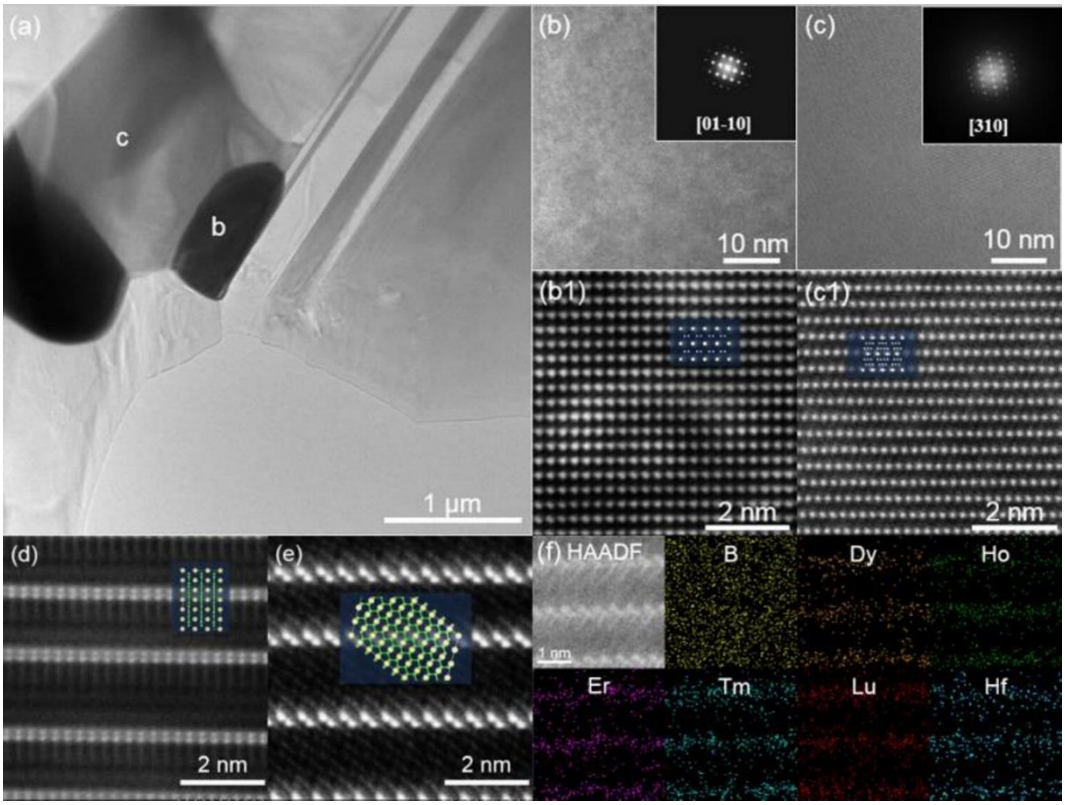

Figure 5. (a) BF-TEM image of grains with FFT in right inset. (b1), (c1), (d), (e) atomic resolved HAADF images, (f) HAADF and EDS. Reprinted with permission from Cui et al. [100]

Zhang et al. [90] have used a sol-gel assisted carbothermal reduction in the case of $(Hf_{0.2}Zr_{0.2}Ti_{0.2}Ce_{0.2}La_{0.2})C$. This method resulted initially a high entropy oxide and later the carbide phase. Hafnium(IV) acetylacetonate, zirconium(IV) acetylacetonate, titanium(IV) isopropoxide, cerium(III) acetylacetonate, and lanthanum(III) acetylacetonate were mixed in benzyl alcohol. The mixture was loaded into an autoclave and was heated to 220 °C for 48 h resulting in a metal oxide precursor, after ethyl ether was used as a gelation agent. The metal oxide precursor was heated to 220 °C for 5 h, resulting in a high entropy oxide which then was mixed with glucose (as a carbon source) and dispersed in water. After pyrolysis at temperatures higher than 1300 °C, it resulted in single-phase high entropy carbides.

The oxides that were synthesized by the sol-gel method were observed to be amorphous up to 400 °C. The sol-gel technique was used to synthesize the compositions $(HfZrTi)O_x$, $(HfZrTiCe)O_x$, $(HfZrTiLa)O_x$ and $(HfZrTiCeLa)O_x$. The similarity in the diffractograms of the synthesized compositions suggests that the mixing entropy had a low effect on nucleation [90]. At higher temperatures, the $(Hf_{0.2}Zr_{0.2}Ti_{0.2}Ce_{0.2}La_{0.2})O_x$ is found to be of fluorite structure and the elements Hf, Zr, Ti, Ce, and La are homogenously distributed with a lattice spacing d_{111} of 0.273 nm.

The presence of glucose as a carbon source resulted in $(Hf_{0.2}Zr_{0.2}Ti_{0.2}Ce_{0.2}La_{0.2})C$ only after pyrolysis at 1600 °C and as the amount of glucose was increased, the secondary phase shifted from La_2O_3 to LaC_2. After carbothermal reduction, both $(Hf_{0.2}Zr_{0.2}Ti_{0.2}Ce_{0.2}La_{0.2})C$ and $(Hf_{0.2}Zr_{0.2}Ti_{0.2}Ce_{0.2}La_{0.2})C$ with an amorphous layer of $(Hf_{0.2}Zr_{0.2}Ti_{0.2}Ce_{0.2}La_{0.2})(O)C$ formed.

$(Nb_{0.25}Ta_{0.25}Ti_{0.25}\ Zr_{0.25})C$ composition [85] was prepared directly via carbothermal reduction of Nb2O5, Ta2O5, TiO2 and ZrO2 at 2000 °C (see Figure 6).

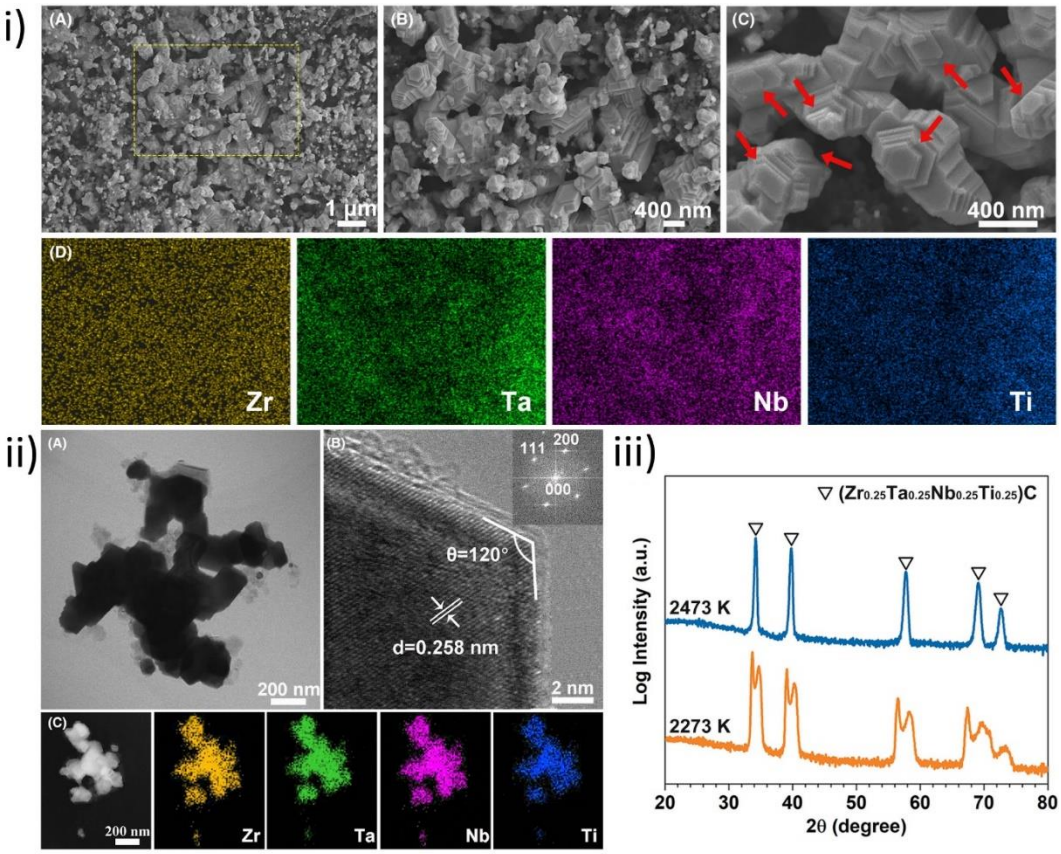

Figure 6. (i) SEM-EDS of coral-shaped $(Nb_{0.25}Ta_{0.25}Ti_{0.25}\ Zr_{0.25})C$. (ii) TEM -EDS and SAED (iii) XRD of the synthesized $(Nb_{0.25}Ta_{0.25}Ti_{0.25}\ Zr_{0.25})C$ at 2000 °C and 2200°C. Reprinted from Ye et al. [85]

Interestingly, $(Mo_{0.2}Nb_{0.2}Ta_{0.2}Ti_{0.2}Zr_{0.2})C$ was synthesized by magnesiothermic carbothermal reduction of ball-milled MoO_3, Nb_2O_5, Ta_2O_5, TiO_2, and ZrO_2 along with graphite and Mg at 1350 °C – the obtained mixture consisting of the high-entropy carbide and magnesium oxide was rinsed with HCl to obtain MgO-free carbide powders (see Figure 6) [67].

3.3 Pressure and Pressureless Sintering or Densification

Generally, the sintering involves two steps, the first step being the mechanical mixing of the respective precursors and the second step being the simultaneous compaction and heating, i.e. reactive sintering. These precursors can either be oxides, metals, or even the binary ceramics themselves.

Gild et al. [77] have synthesized several diboride ceramics, namely $(Hf_{0.2}Zr_{0.2}Ta_{0.2}Nb_{0.2}Ti_{0.2})B_2$, $(Hf_{0.2}Zr_{0.2}Ta_{0.2}Mo_{0.2}Ti_{0.2})B_2$, $(Hf_{0.2}Zr_{0.2}Mo_{0.2}Nb_{0.2}Ti_{0.2})B_2$, $(Hf_{0.2}Mo_{0.2}Ta_{0.2}Nb_{0.2}Ti_{0.2})B_2$, $(Mo_{0.2}Zr_{0.2}Ta_{0.2}Nb_{0.2}Ti_{0.2})B_2$, and $(Hf_{0.2}Zr_{0.2}Ta_{0.2}Cr_{0.2}Ti_{0.2})B_2$ by combined sintering of individual binary metal borides. The metal borides were ball-milled under Argon. The obtained ball-milled mixture was sintered at 2000 °C for 5 min with 30 MPa resulting in a single-phase phase AlB_2-type structure (see Figure 7). A Mo foil was used as an intermittent to prohibit the reaction between the powders and the graphite crucible. Also, Qin et al. [74] have synthesized $(Ti_{0.2}Zr_{0.2}Hf_{0.2}Mo_{0.2}W_{0.2})B_2$, $(Ti_{0.2}Ta_{0.2}Cr_{0.2}Mo_{0.2}W_{0.2})B_2$, $(Zr_{0.2}Hf_{0.2}Nb_{0.2}Ta_{0.2}W_{0.2})B_2$, and $(Zr_{0.225}Hf_{0.225}Ta_{0.225}Mo_{0.225}W_{0.1})B_2$ from elements through reactive sintering. The individual elements were ball milled with boron, using stearic acid as a lubricant, and were sintered in two steps, similar to the method reported by Tallarita et al. [7] The die was held at 1400 °C and 1600 °C to promote the reactions of boron with oxides as well as simultaneously occurring outgassing. Later, they were sintered at 2000 °C, resulting in a complete single phase with W and Mo being stabilized without segregations at high temperatures.

Kavak et al. [75] have synthesized quaternary diboride $(Hf_{0.25}Ti_{0.25}W_{0.25}Zr_{0.25})B_2$ in mechanochemistry-assisted SPS. The HfO_2, TiO_2, ZrO_2, and WO_3 were reacted individually with boron using magnesiothermic reactions. The obtained binary diborides were then milled along with boron under Ar with a pause of 5 min after each finished 60 min of a total milling time of 4-10 h. The obtained milled powder was sintered at 1800 °C-2050 °C to obtain a single-phase diboride with minor oxide impurities.

Qin et al. [8], [70], [72], [74] have synthesized various tetraboride compositions, i.e., $(Y_{0.17}Nd_{0.18}Sm_{0.21}Gd_{0.22}Er_{0.22})B_4$, $(Y_{0.21}Sm_{0.19}Gd_{0.21}Er_{0.18}Yb_{0.21})B_4$, $(Y_{0.22}La_{0.18}Pr_{0.20}Dy_{0.23}Er_{0.17})B_4$, $(Y_{0.22}Nd_{0.18}Gd_{0.20}Dy_{0.21}Er_{0.19})B4$, $(Y_{0.22}Nd_{0.20}Sm_{0.20}Gd_{0.19}Tb_{0.19})B_4$ and $(Nd_{0.18}Sm_{0.19}Gd_{0.23}Tb_{0.21}Yb_{0.19})B_4$ as well as hexaborides with lanthanides, obtaining relative densities of at least 98% for the compositions $(Y_{0.23}Nd_{0.21}Sm_{0.20}Gd_{0.18}Yb_{0.18})B_6$, $(Y_{0.19}La_{0.19}Pr_{0.22}Dy_{0.19}Yb_{0.21})B_6$, $(La_{0.19}Nd_{0.21}Sm_{0.23}Gd_{0.19}Yb_{0.18})B_6$, $(Y_{0.22}La_{0.20}Nd_{0.19}Sm_{0.22}Gd_{0.17})B_6$, $(Y_{0.21}La_{0.17}Nd_{0.18}Sm_{0.21}Tb_{0.23})B_6$ and $(La_{0.18}Pr_{0.21}Nd_{0.19}Sm_{0.21}Tb_{0.21})B_6$. [8] Compared to the procedure of Gild et al. [77], who performed SPS of the ball-milled mixture of metallic powders and boron, the parameters differ, as 1700 °C with a pressure of 50 MPa and a holding time of 10 min were used by Qin et al. The compacted powders were then sintered to obtain single-phase ceramics. Through this process, M_3B_4-based high entropy borides of compositions $(V_{0.2}Cr_{0.2}Nb_{0.2}Mo_{0.2}Ta_{0.2})_3B_4$ and $(V_{0.2}Cr_{0.2}Nb_{0.2}Ta_{0.2}W_{0.2})_3B_4$ were synthesized, which showed minor impurities in form of M_5B_6 phase [71]. Also, various high-entropy monoboride compositions, i.e., $(V_{0.2}Cr_{0.2}Nb_{0.2}Ta_{0.2}W_{0.2})B$, $(V_{0.2}Cr_{0.2}Nb_{0.2}Mo_{0.2}W_{0.2})B$ and $(V_{0.2}Cr_{0.2}Nb_{0.2}Mo_{0.2}Ta_{0.2})B$, were synthesized via reactive sintering with similar conditions [2].

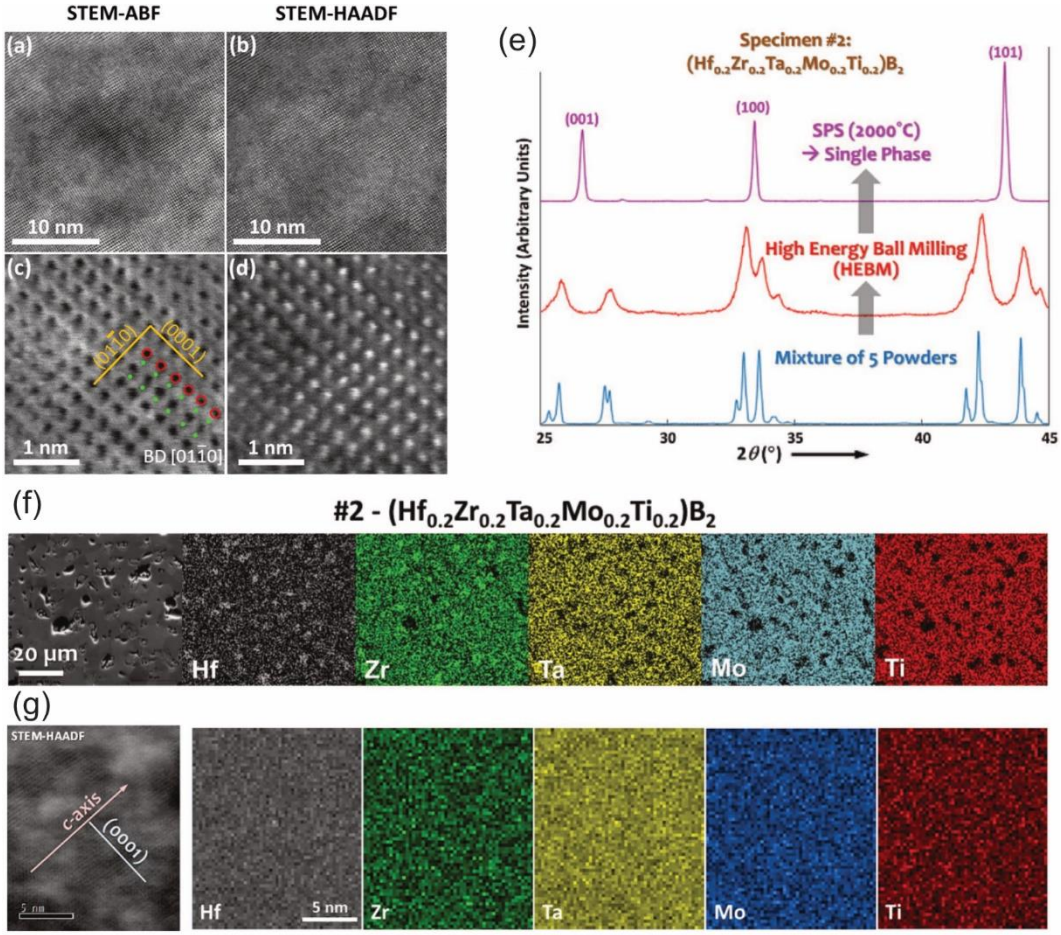

Figure 7. Structural characterization of $(Hf_{0.2}Zr_{0.2}Ta_{0.2}Mo_{0.2}Ti_{0.2})B_2$. (a), (b) ABF and HAADF, (c), (d) ABF and HAADF at higher magnification showing the cations (in red) and boron (in green) (e) XRD of $(Hf_{0.2}Zr_{0.2}Ta_{0.2}Mo_{0.2}Ti_{0.2})B_2$ at different stages of synthesis (f), (g) SEM EDS and STEM EDS of $(Hf_{0.2}Zr_{0.2}Ta_{0.2}Mo_{0.2}Ti_{0.2})B_2$. Reprinted from Gild et al. [77]

In the case of some carbide-based UHTC compositions [43], a unique route of non-reactive sintering was found. The cold-pressed green bodies of carbides were placed in an electro-resistively heated graphite felt in an argon atmosphere. Rapid heating of the cold-pressed green body leads to sintering. Although the current and heating are prone to be uneven, the process proved to be a fast and energy-efficient way to obtain dense ceramic pellets.

Dippo et al. [16] prepared several bulk high entropy (carbo)nitrides by performing SPS of milled binary nitrides and carbides under vacuum at 2000 °C. Further, Moskovskikh et al. [50] have synthesized high entropy nitrides with combustion synthesis-assisted SPS. The high energy ball milled metallic powders were combusted under N_2 of 8 atm pressure. The obtained nitride powders were then sintered at 1800 °C for 20 min with a pressure of 30 MPa under 0.8 atm N_2 (see Figure 8).

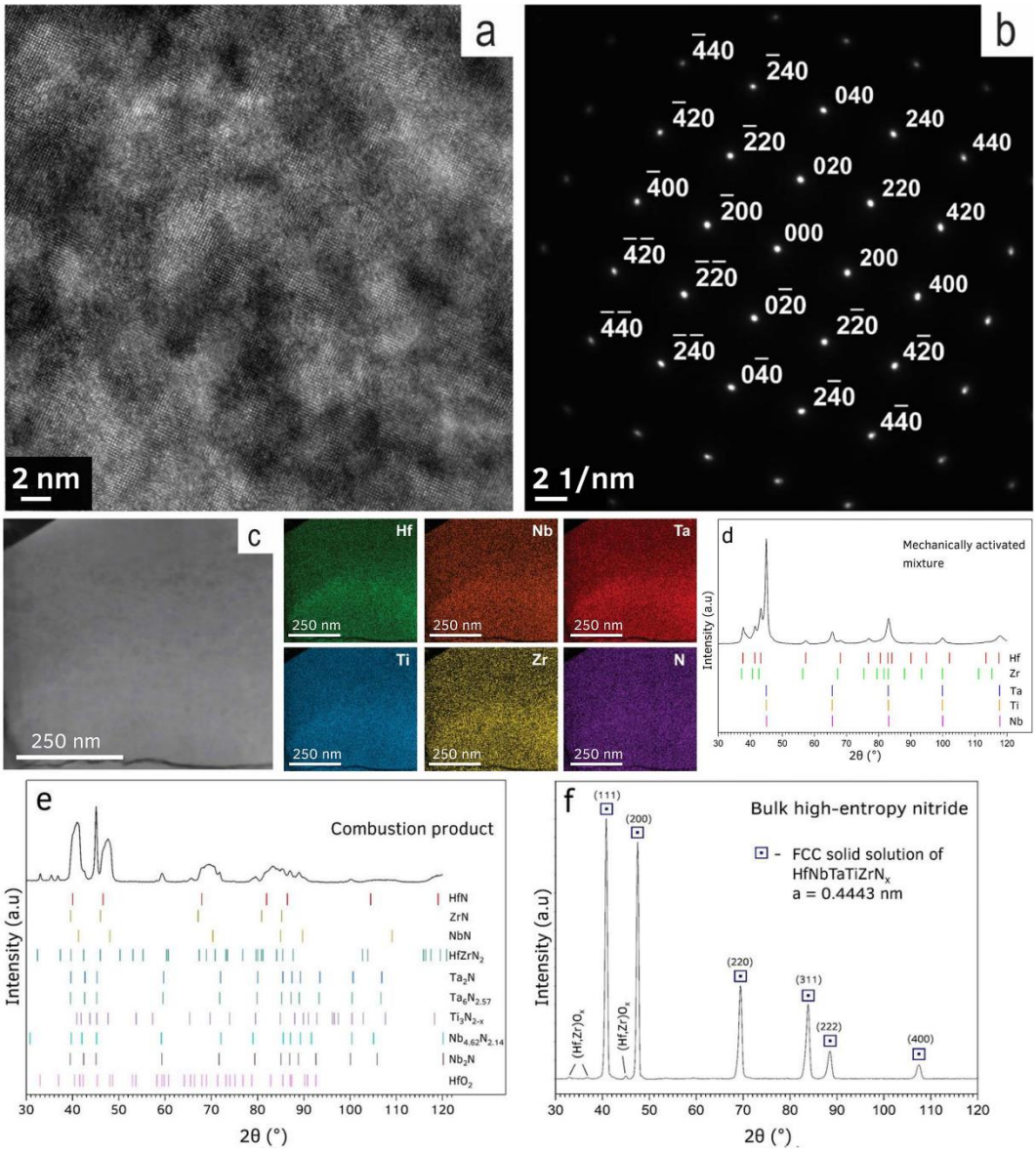

Figure 8. (a) HRTEM of $(Hf_{0.2}Ta_{0.2}Ti_{0.2}Nb_{0.2}Zr_{0.2})N$, (b) SAED pattern from [001] zone axis, (c) EDS mapping (d), (e), (f) XRD of the precursors at different stages of the synthesis. Reprinted from Moskovskikh et al. [50]

High-entropy silicides of $(V_{0.2}Cr_{0.2}Nb_{0.2}Ta_{0.2}W_{0.2})_5Si_3$ and $(Ti_{0.2}Zr_{0.2}Nb_{0.2}Mo_{0.2}Hf_{0.2})_5Si_3$ have been prepared by Sivakumar et al. [87] in ball-milled assisted SPS at 1900 °C and 1800 °C respectively, with a holding time of 20 min at 50 MPa. Interestingly, these phases were found to be of Mn_5Si_3-type hexagonal $D8_8$ structure, although the binary V, Cr, Nb, Ta, and W silicides exhibit rather tetragonal Cr_5Si_3 ($D8_1$) or W_5Si_3 ($D8_m$).

Composition $(Zr_{0.196}Hf_{0.02}V_{0.196}Nb_{0.196}Mo_{0.196}W_{0.196})C_x$ was synthesized by the Hot-pressing route by Zhang et al. [110] by ball milling the oxides with carbon for 20 h and subsequent carbothermal reduction at 1600 °C for 1 hr in a vacuum and hot pressed at 2100 °C for 60 min with the pressure of 30 MPa resulting in single phase carbide at x = 0.7 and 0.8 and the rest compositions had either spinodal decomposition or discontinuous precipitation.

3.4 Molten Salt

Molten salt synthesis was employed recently by Ning et al. for a medium entropic ceramic $(Ta_{0.25}Ti_{0.25}Nb_{0.25}V_{0.25})C$ [64]. The elements Ta, Ti, V, and Nb along with carbon were mixed in KCl and resulted in $(Ta_{0.25}Ti_{0.25}V_{0.25}Nb_{0.25})C$ ceramic without any oxidic impurities after pyrolysis under argon at 1300 °C (see Figure 9).

$(Ta_{0.25}Hf_{0.25}Ti_{0.25}Nb_{0.25})Si_2$ was prepared via the molten salt method using transition metal oxides. Thus, Ta_2O_5, HfO_2, TiO_2, and Nb_2O_5 were mixed along with 200 wt% excess SiO_2 as well as 350-400 wt% excess Mg and NaCl+KCl. The mixture was pyrolyzed under argon at 800 °C for 6 h, resulting in fine disilicide powders [88].

Ye [89] used metal oxides, B_2O_3, $MgCl_2$ and Mg for the magnesio-thermic synthesis of $(Zr_{0.25}Ta_{0.25}Nb_{0.25}Ti_{0.25})B_2$, $(Hf_{0.25}Ta_{0.25}Nb_{0.25}Ti_{0.25})B_2$, $(Hf_{0.25}Zr_{0.25}Ta_{0.25}Nb_{0.25})B_2$ and $(Ta_{0.25}Nb_{0.25}Ti_{0.25}Cr_{0.25})B_2$. As the compositionally complex ceramics supersaturate the molten salt, the fine-grained ceramics with a particle size well below 100 nm can be obtained (see Figure 9).

The underlying mechanism in a molten salt-assisted synthesis is the dissolution of cation precursors into the molten salt, causing an intermediate state where cations and delocalized electrons are present. These delocalized electrons then are accepted by the dissolved anionic precursor, resulting in delocalized anions. The recombination of the ions at the anionic surface leads to the formation of a high-entropy ceramic [64].

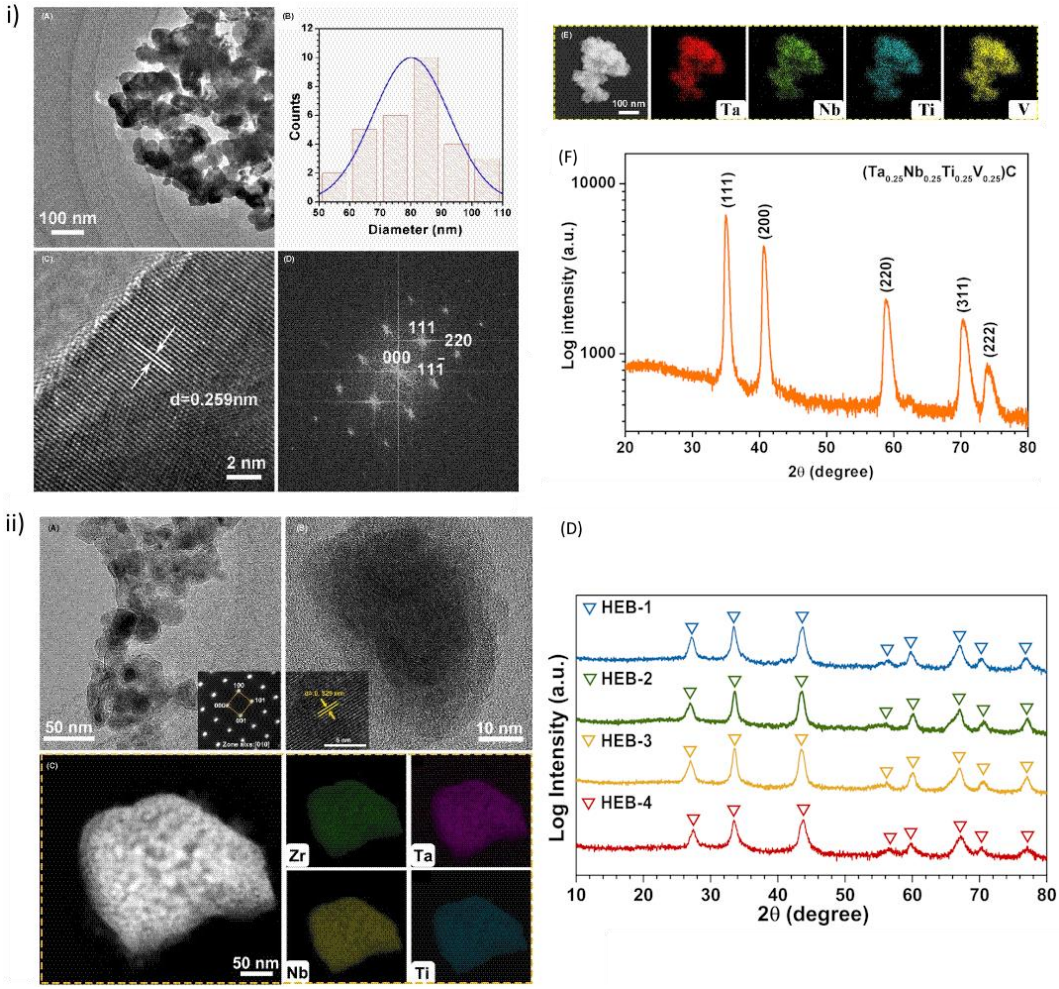

Figure 9. i) (A), (C) TEM, (B) particle size distribution, (D) SAED, (E) EDS mapping, (F) XRD of $(Ta_{0.25}Ti_{0.25}V_{0.25}Nb_{0.25})C$. Reprinted from Ning et al. [64]. ii) (A)-(C) TEM with SAED and EDS and (D) XRD of $(Zr_{0.25}Ta_{0.25}Nb_{0.25}Ti_{0.25})B_2$. Reprinted from Ye et al. [89]

3.5 Sol-Gel

The sol-gel process is a wet chemical synthesis route starting from a solution in either water, organic solvents, or a combination thereof, that is, through condensation and hydrolysis, forming a network with an enclosed solvent, a gel, depicted in Figure 10. It mostly is straightforward, without any complicated setup or processing involved – with some exceptions being supercritical drying to obtain aerogels or oxygen-free syntheses. This process can be applied to a good number of ceramic classes, such as borides, carbides, oxides, and many more. Yang et al. [63] have produced $(Cr_{0.2}Hf_{0.2}Mo_{0.2}Nb_{0.2}Ta_{0.2})B_2$ for which $HfCl_4$, $NbCl_5$, $CrCl_3.6H_2O$, Mo(II)acetylacetonate and $TaCl_5$ were dissolved in ethanol. Further, sorbitol and boric acid were mixed along with citric acid and ethylene glycol into the solution, which was heated and dried to obtain a xerogel. It was later pyrolyzed under argon resulting in a high entropy diboride powder. The sol-gel route was further used by [31] to obtain a high entropy carbide sample. [31] used the respective chlorides with the furfuryl alcohol as the gel former with butanol as the solvent, obtaining a gel which later, upon pyrolysis, resulted in a single-phase high entropy carbide. Usually, the precursor needs to feature carbon-rich functional groups, e.g., alcohol. Other precursors such as citric acid, glucose, and PEG along with water-soluble salts can be considered to obtain the target compositionally complex ceramics at high temperatures. Interestingly, this method was modified by [96] by substituting alcohols with acetyl methane and butanol and then reacting the mixture in a hydrothermal autoclave chamber to obtain the gel which after pyrolysis results in carbide.

For nitrides, however, the reaction only involved one step in which the chlorides react with urea to form metal urea gels, which later are pyrolyzed to obtain the nitride ceramics (see Figure 11). [29],[69]

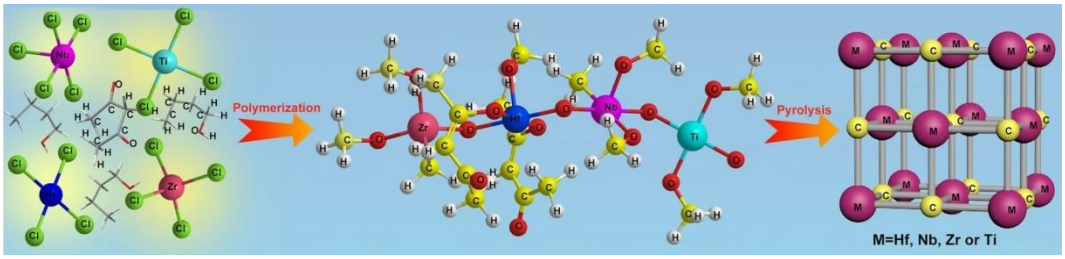

Figure 10. Schematic diagram of the sol-gel process in the case of high entropy carbides. Reprinted from Du et al. [56]

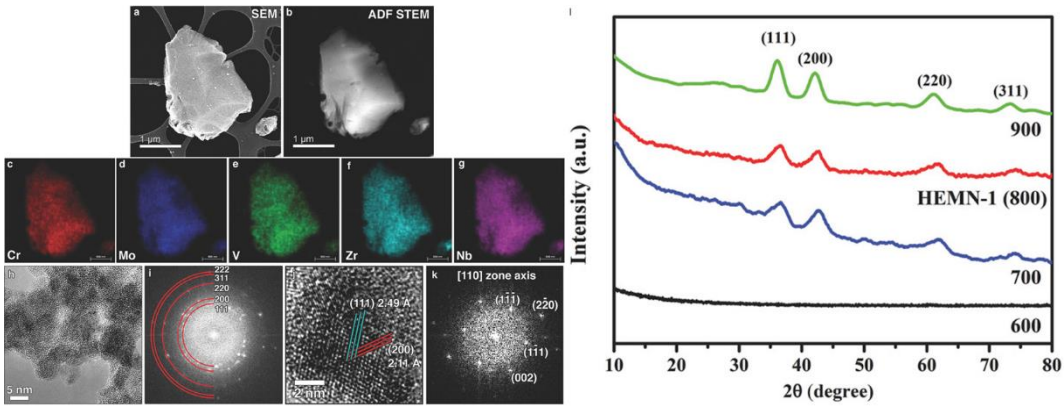

Figure 11. (a) SEM, (b-k) TEM with EDS and SAED and (l) XRD of $(Cr_{0.2}Mo_{0.2}V_{0.2}Zr_{0.2}Nb_{0.2})N$. Reprinted from Jin et al. [29]

3.6 Arc-Melting

The arc melting method involves the melting of the respective individual ceramics into a homogenized solution and later cooling to obtain homogenous high entropy ceramics. However, this method cannot be used for nitrides and other materials with high vapor pressure. As carbides and borides possess significantly lower vapor pressure, there are many studies involving these material classes. In [92], a quinary and four quaternary compositions of the (Hf, Ta, Ti, Zr, Cr)B_2 family, were obtained as single-phase compounds in all the compositions. However, the chromium-containing samples showed a decreased amount of chromium due to its relatively low melting point and high vapor pressure when compared to other borides.

For carbides, Ya et al. [62] used oxides and graphite as precursors to react them under DC arc discharge and subsequently used the resulting binary carbides to form a high entropy carbide solid solution through a further arc-melting step

In the case of Xia et al. [93], ball-milled binary carbides were directly arc melted to obtain the ceramic $(Nb_{0.25}Mo_{0.25}Ta_{0.25}W_{0.25})C$ and $(Nb_{0.2}Mo_{0.2}Ta_{0.2}W_{0.2}Hf_{0.2})C$.

3.7 High Pressure and High-Temperature Compaction/Sintering

Recently, the synthesis of high-entropy ceramics has also been realized through high-pressure high-temperature techniques. Guan et al. [14], [94], prepared the well-known $(Ti_{0.2}Zr_{0.2}Nb_{0.2}Ta_{0.2}Mo_{0.2})C$ and $(Hf_{0.2}Nb_{0.2}Ta_{0.2}Ti_{0.2}Zr_{0.2})C$ and phases by pressurizing the powder mixtures of the binary carbides to 5.5 GPa and simultaneously heating them to 1600-2000 °C, resulting in single-phase high entropy carbides.

Iwan et al. [97,99] synthesized $(Hf_{0.2}Ti_{0.2}Zr_{0.2}Ta_{0.2}Mo_{0.2})B_2$ via high-pressure high-temperature reactions (see Figure 12). The materials used were the oxides of the respective metals, i.e. HfO_2, TiO_2, ZrO_2, Ta_2O_5, and MoO_3, as well as slightly excess B_4C and C to diminish the retention of oxides at the synthesis conditions, compensating the loss of B and C as B_2O_3 and CO respectively. All powders were thoroughly milled before loading them into the high-pressure cell.

$(Hf_{0.2}Mo_{0.2}Nb_{0.2}Ta_{0.2}Ti_{0.2})B_2$ and $(Hf_{0.2}Mo_{0.2}Nb_{0.2}Ti_{0.2}Zr_{0.2})B_2$ were synthesized analogously, the setup is schematically shown in Figure 13.[97] The high entropy borides formed at a pressure of 0.9 GPa at temperatures above 1100 °C and were measured up to 9.5 GPa and 2000 °C (see Figure 14).

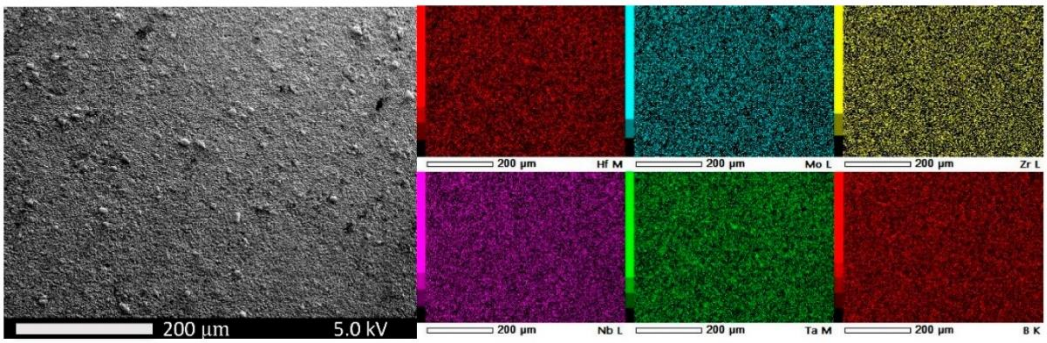

Figure 12. SEM micrographs of $(Hf_{0.2}Mo_{0.2}Zr_{0.2}Nb_{0.2}Ta_{0.2})B_2$. Reprinted from Iwan et el. [99]

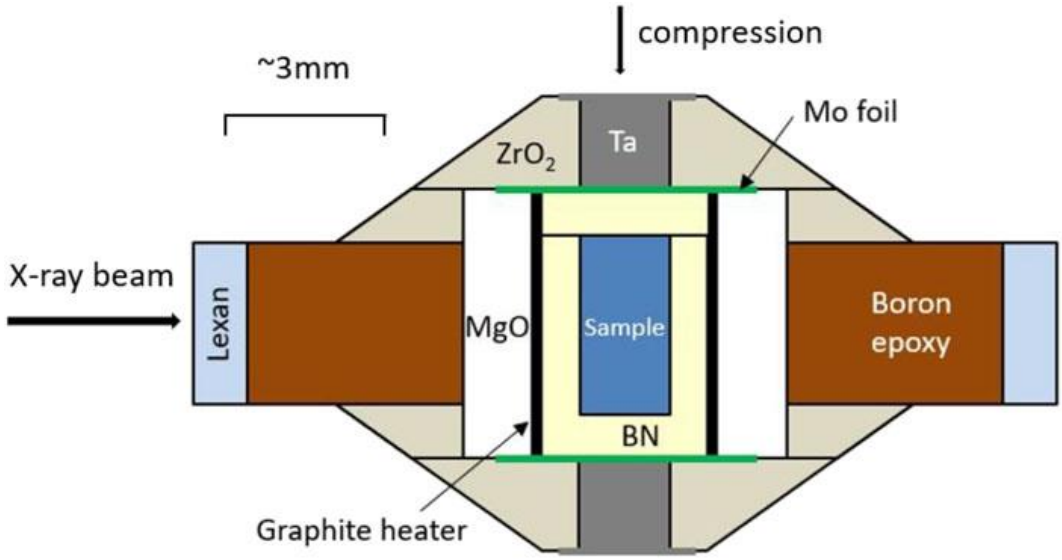

Figure 13. Schematic of a general HP-HT used by Iwan et al. up to 7.6 GPa and 1600 °C. [97]

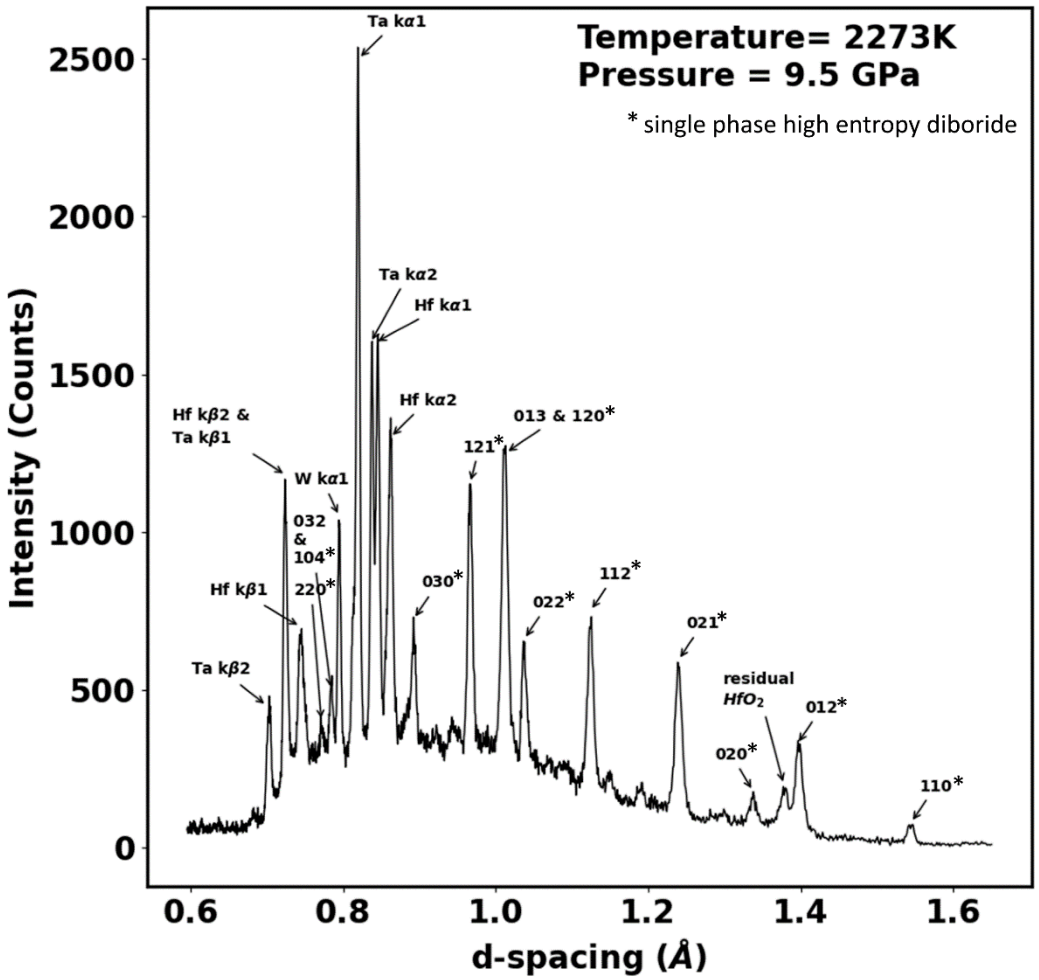

Figure 14. XRD of $(Hf_{0.2}Mo_{0.2}Nb_{0.2}Ta_{0.2}Ti_{0.2})B_2$. Reprinted from Iwan et el. [99].

All compositions up to date that were successfully synthesized as single phase including minor oxidic impurities are listed below in Table 1. The borides, especially diborides triggered the motivation of looking for UHTCs with improved ultrahigh temperature capability. The number of synthesized compositionally complex carbides is markedly high, indicating that their preparative access is less difficult- this possibly relies on their robust process (typically carbothermal reactions of oxides) as well as the high thermodynamic stability in this class of materials. The nitrogen fugacity in the materials at the temperatures of synthesis and processing results in difficulties during the preparations, due to which the number of synthesized carbonitrides and nitrides is less.

Table 1. Synthesized compositions of UHT-CCC and their crystal structures

Ceramic	Synthesized compositions	Crystal structure	Reference
Mono-borides	$(Cr_{0.2}Mo_{0.2}Nb_{0.2}\ V_{0.2}W_{0.2})B$	*Cmcm*	[2]
	$(Cr_{0.2}Mo_{0.2}Ni_{0.2}\ V_{0.2}W_{0.2})B$		[59]
	$(Cr_{0.2}\ Mo_{0.2}Nb_{0.2}Ta_{0.2}V_{0.2})B$		[2]
	$(Cr_{0.2}Mo_{0.2}Ta_{0.2}Ni_{0.2}W_{0.2})B$		[59],[60]
	$(Cr_{0.2}Nb_{0.2}Ta_{0.2}V_{0.2}W_{0.2})B$		[2]
	$(V_{0.2}Mo_{0.2}W_{0.2}Nb_{0.2}Ni_{0.2})B$		[59]
	$(V_{0.2}Cr_{0.2}Mo_{0.2}W_{0.2}Ti_{0.2})B$		[59]
	$(V_{0.2}Mo_{0.2}Ta_{0.2}Ni_{0.2}W_{0.2})B$		[59]
Di-borides	$(Hf_{0.333}Ti_{0.333}Zr_{0.333})B_2$	*P6/mmm*	[65]
	$(Cr_{0.25}Nb_{0.25}Ta_{0.25}Ti_{0.25})B_2$		[89]
	$(Hf_{0.25}Nb_{0.25}Ta_{0.25}Ti_{0.25})B_2$		[89]
	$(Hf_{0.25}Nb_{0.25}Ta_{0.25}Zr_{0.25})B_2$		[89]
	$(Hf_{0.25}Sc_{0.25}Ta_{0.25}Zr_{0.25})B_2$		[91]
	$(Hf_{0.25}Ti_{0.25}V_{0.25}Zr_{0.25})B_2$		[109]
	$(Hf_{0.25}Ti_{0.25}W_{0.25}Zr_{0.25})B_2$		[75]
	$(Nb_{0.25}Ta_{0.25}Ti_{0.25}Zr_{0.25})B_2$		[89]
	$(Hf_{0.25}Ta_{0.25}Ti_{0.25}Zr_{0.25})B_2$		[92]
	$(Cr_{0.25}Hf_{0.25}Ti_{0.25}Zr_{0.25})B_2$		[92]
	$(Cr_{0.25}Hf_{0.25}Ta_{0.25}Zr_{0.25})B_2$		[92]
	$(Cr_{0.25}Hf_{0.25}Ta_{0.25}Ti_{0.25})B_2$		[92]
	$(Cr_{0.25}Ta_{0.25}Ti_{0.25}Zr_{0.25})B_2$		[92]
	$(Hf_{0.28}Zr_{0.28}Ta_{0.28}W_{0.15})B_2$		[103]
	$(Cr_{0.2}Hf_{0.2}Mo_{0.2}Nb_{0.2}Ta_{0.2})B_2$		[63]
	$(Cr_{0.2}Hf_{0.2}Ta_{0.2}Ti_{0.2}Zr_{0.2})B_2$		[74],[92]
	$(Cr_{0.2}Mo_{0.2}Ta_{0.2}Ti_{0.2}W_{0.2})B_2$		[74]
	$(Er_{0.2}Hf_{0.2}Ta_{0.2}Ti_{0.2}Zr_{0.2})B_2$		[108]
	$(Hf_{0.2}Mo_{0.2}Nb_{0.2}Ta_{0.2}Ti_{0.2})B_2$		[7],[77],[99]
	$(Hf_{0.2}Mo_{0.2}Nb_{0.2}Ti_{0.2}Zr_{0.2})B_2$		[77]
	$(Hf_{0.2}Mo_{0.2}Nb_{0.2}Ta_{0.2}Zr_{0.2})B_2$		[99]
	$(Hf_{0.2}Mo_{0.2}Ta_{0.2}Ti_{0.2}Zr_{0.2})B_2$		[77],[97]
	$(Hf_{0.2}Mo_{0.2}Ti_{0.2}W_{0.2}Zr_{0.2})B_2$		[74]
	$(Hf_{0.2}Nb_{0.2}Ta_{0.2}Ti_{0.2}Zr_{0.2})B_2$		[77]
	$(Hf_{0.2}Nb_{0.2}Ta_{0.2}V_{0.2}Zr_{0.2})B_2$		[10]
	$(Hf_{0.2}Nb_{0.2}Ta_{0.2}W_{0.2}Zr_{0.2})B_2$		[74]
	$(Mo_{0.2}Nb_{0.2}Ta_{0.2}Ti_{0.2}Zr_{0.2})B_2$		[77]
	$(Zr_{0.225}Hf_{0.225}Ta_{0.225}Mo_{0.225}W_{0.1})B_2$		[74]
Tetra-borides	$(Y_{0.17}Nd_{0.18}Sm_{0.21}Gd_{0.22}Er_{0.22})B_4$	*P4/mbm*	[72]
	$(Y_{0.21}Sm_{0.19}Gd_{0.21}Er_{0.18}Yb_{0.21})B_4$		[72]
	$(Y_{0.22}La_{0.18}Pr_{0.20}Dy_{0.23}Er_{0.17})B_4$		[72]
	$(Y_{0.22}Nd_{0.18}Gd_{0.20}Dy_{0.21}Er_{0.19})B_4$		[72]
	$Y_{0.22}Nd_{0.20}Sm_{0.20}Gd_{0.19}Tb_{0.19})B_4$		[72]
	$(Nd_{0.18}Sm_{0.19}Gd_{0.23}Tb_{0.21}Yb_{0.19})B_4$		[72]
Hexa-borides	$(Y_{0.23}Nd_{0.21}Sm_{0.20}Gd_{0.18}Yb_{0.18})B_6$	*Pm-3m*	[8]
	$(Y_{0.19}La_{0.19}Pr_{0.22}Dy_{0.19}Yb_{0.21})B_6$		[8]
	$(La_{0.19}Nd_{0.21}Sm_{0.23}Gd_{0.19}Yb_{0.18})B_6$		[8]
	$(Y_{0.22}La_{0.20}Nd_{0.19}Sm_{0.22}Gd_{0.17})B_6$		[8]
	$(Y_{0.21}La_{0.17}Nd_{0.18}Sm_{0.21}Tb_{0.23})B_6$		[8]
	$(La_{0.18}Pr_{0.21}Nd_{0.19}Sm_{0.21}Tb_{0.21})B_6$		[8]

Ceramic	Synthesized compositions	Crystal structure	Reference
M_3B_4	$(V_{0.2}Cr_{0.2}Nb_{0.2}Mo_{0.2}Ta_{0.2})_3B_4$	*Immm*	[71]
	$(V_{0.2}Cr_{0.2}Nb_{0.2}Ta_{0.2}W_{0.2})_3B_4$		[71]
Dodeca-borides	$(Dy_{0.166}Ho_{0.166}Er_{0.166}Tm_{0.166}Lu_{0.166}Hf_x)B_{12}$	*Fm*-3*m*(UB_{12})	[100]
	$(Dy_{0.2}Ho_{0.2}Er_{0.2}Tm_{0.2}Lu_{0.2})B_{12}$		[101]
Carbides	$(Hf_{0.333}Ti_{0.333}Zr_{0.333})C$		[105]
	$(Nb_{0.333}Ta_{0.333}Zr_{0.333})C$		[95],[106]
	$(Ta_{0.333}Ti_{0.333}Zr_{0.333})C$		[86]
	$(Hf_{0.25}Nb_{0.25}Ta_{0.25}Zr_{0.25})C$		[39],[47]
	$(Hf_{0.25}Ta_{0.25}Ti_{0.25}Zr_{0.25})C$		[44]
	$(Mo_{0.25}Nb_{0.25}Ta_{0.25}W_{0.25})C$		[93]
	$(Nb_{0.25}Ta_{0.25}Ti_{0.25}\ Zr_{0.25})\ C$		[13],[57],[85],[96]
	$(Nb_{0.25}\ Ta_{0.25}Ti_{0.25}V_{0.25})C$		[24],[64]
	$(Nb_{0.25}Ti_{0.25}V_{0.25}Zr_{0.25})C$		[80]
	$(Ce_{0.2}Hf_{0.2}La_{0.2}Ti_{0.2}Zr_{0.2})C$		[90]
	$(Cr_{0.2}Nb_{0.2}Ta_{0.2}Ti_{0.2}V_{0.2})C$		[43]
	$(Cr_{0.2}Nb_{0.2}Ta_{0.2}Ti_{0.2}Zr_{0.2})C$		[43]
	$(Cr_{0.2}Nb_{0.2}Ti_{0.2}V_{0.2}Zr_{0.2})C$		[43]
	$(Hf_{0.2}Mo_{0.2}Nb_{0.2}Ta_{0.2}Ti_{0.2})C$		[41]
	$(Hf_{0.2}Mo_{0.2}Nb_{0.2}Ta_{0.2}W_{0.2})C$		[93]
	$(Hf_{0.2}Mo_{0.2}Ta_{0.2}Ti_{0.2}Zr_{0.2})C$		[41]
	$(Hf_{0.2}Nb_{0.2}Ta_{0.2}Ti_{0.2}V_{0.2})C$	*Fm*-3*m*	[26],[30]
	$(Hf_{0.2}Nb_{0.2}Ta_{0.2}Ti_{0.2}W_{0.2})C$		[41]
	$(Hf_{0.2}Nb_{0.2}Ta_{0.2}Ti_{0.2}Zr_{0.2})C$		[30],[57]
	$(Hf_{0.2}Nb_{0.2}Ta_{0.2}V_{0.2}Zr_{0.2})C$		[26]
	$(Hf_{0.2}Nb_{0.2}Ti_{0.2}V_{0.2}Zr_{0.2})C$		[26]
	$(Hf_{0.2}Ta_{0.2}Ti_{0.2}V_{0.2}Zr_{0.2})C$		[26]
	$(Hf_{0.2}Ta_{0.2}Ti_{0.2}W_{0.2}Zr_{0.2})C$		[30]
	$(Mo_{0.2}Nb_{0.2}Ta_{0.2}Ti_{0.2}V_{0.2})C$		[41]
	$(Mo_{0.2}Nb_{0.2}Ta_{0.2}Ti_{0.2}Zr_{0.2})C$		[57]
	$(Mo_{0.2}Nb_{0.2}Ta_{0.2}V_{0.2}W_{0.2})C$		[30],[45]
	$(Nb_{0.2}Ta_{0.2}Ti_{0.2}V_{0.2}W_{0.2})C$		[30]
	$(Nb_{0.2}Ta_{0.2}Ti_{0.2}V_{0.2}Zr_{0.2})C$		[30]
	$(Nb_{0.2}Ta_{0.2}Ti_{0.2}W_{0.2}Zr_{0.2})C$		[96]
	$(Zr_{0.196}Hf_{0.02}V_{0.196}Nb_{0.196}Mo_{0.196}W_{0.196})C_x$		[110]
	$(Cr_{0.16}Nb_{0.16}Ta_{0.16}Ti_{0.16}V_{0.16}Zr_{0.16})C$		[43]
	$(Hf_{0.16}Nb_{0.16}Ta_{0.16}Ti_{0.16}W_{0.16}Zr_{0.16})C$		[96]
	$(Ti_{0.16}Zr_{0.16}Hf_{0.16}Nb_{0.16}Ta_{0.16}Mo_{0.16})C$		[19]
	$(Cr_{0.143}\ Mo_{0.143}\ Nb_{0.143}Ta_{0.143}Ti_{0.143}V_{0.143}\ Zr_{0.143})C$		[43]
	$(Hf_{0.143}Nb_{0.143}Ta_{0.143}Ti_{0.143}V_{0.143}W_{0.143}Zr0_{.143})C$		[96]
	$(Cr_{0.125}\ Mo_{0.125}Nb_{0.125}Ta_{0.125}\ Ti_{0.125}V_{0.125}W_{0.125}\ Zr_{0.125})C$		[43]
	$(Hf_{0.125}Mo_{0.125}Nb_{0.125}Ta_{0.125}Ti_{0.125}V_{0.125}W_{0.125}Zr_{0.125})C$		[96]
	$(Ti_{0.11}\ Zr_{0.11}\ Hf_{0.11}\ V_{0.11}\ Nb_{0.11}\ Ta_{0.11}\ Cr_{0.11}\ Mo_{0.11}W_{0.11})C$		[111]

Ceramic	Synthesized compositions	Crystal structure	Reference
(Carbo)-nitrides	$(Ti_{0.333}Zr_{0.333}Hf_{0.333})CN$	*Fm*-3*m*	[102]
	$(Ti_{0.25}Zr_{0.25}Hf_{0.25}Nb_{0.25})CN$		[102]
	$(Hf_{0.2}Nb_{0.2}Ta_{0.2}Ti_{0.2}Zr_{0.2})N$		[50]
	$(Cr_{0.2}Mo_{0.2}Ta_{0.2}V_{0.2}W_{0.2})CN$		[16]
	$(Cr_{0.2}Hf_{0.2}Ta_{0.2}Nb_{0.2}Ti_{0.2})CN$		[16]
	$(Cr_{0.2}Nb_{0.2}Ta_{0.2}Ti_{0.2}V_{0.2})CN$		[16]
	$(V_{0.2}Nb_{0.2}Cr_{0.2}Mo_{0.2}Zr_{0.2})N$		[29]
	$(Cr_{0.2}Nb_{0.2}Ti_{0.2}Ta_{0.2}V_{0.2})N$		[16]
	$(Cr_{0.2}Hf_{0.2}Nb_{0.2}Ta_{0.2}Ti_{0.2})N$		[16]
	$(Hf_{0.2}Ta_{0.2}Nb_{0.2}Zr_{0.2}V_{0.2})N$		[69]
	$(Ti_{0.2}Zr_{0.2}Hf_{0.2}Nb_{0.2}Ta_{0.2})$ CN		[102]
	$(Ti_{0.25}W_{0.25}V_{0.25}Ta_{0.25})N$		[107]
Silicides	$(V_{0.2}Cr_{0.2}Nb_{0.2}Ta_{0.2}W_{0.2})_5Si_3$	*P*6$_3$/*mcm*	[87]
	$(Ti_{0.2}Zr_{0.2}Nb_{0.2}Mo_{0.2}Hf_{0.2})_5Si_3$		[87]
	$(Cr_{0.2}Mo_{0.2}Ta_{0.2}V_{0.2}Nb_{0.2})Si_2$	*P*6$_2$22	[61]
	$(Mo_{0.2}Nb_{0.2}Ta_{0.2}Ti_{0.2}Zr_{0.2})Si_2$		[61]
	$(Ti_{0.2}Zr_{0.2}Nb_{0.2}Mo_{0.2}W_{0.2})Si_2$		[61]
	$(Mo_{0.2}Nb_{0.2}Ta_{0.2}Ti_{0.2}W_{0.2})Si_2$		[61]
	$(Mo_{0.2}W_{0.2}Cr_{0.2}Ta_{0.2}Nb_{0.2})Si_2$		[61]
	$(Nb_{0.25}Ta_{0.25}Hf_{0.25}Ti_{0.25})Si_2$		[88]
Boro-carbo-nitrides	$(Ta_{0.2}Nb_{0.2}Zr_{0.2}Hf_{0.2}W_{0.2})BCN$	*Fm*-3*m*	[18]
	$(Ta_{0.2}Nb_{0.2}Zr_{0.2}Hf_{0.2}Ti_{0.2})BCN$		[18]
	$(Ta_{0.2}Nb_{0.2}Zr_{0.2}Ti_{0.2}W_{0.2})BCN$		[18]

4. Conclusion

Recent studies on the various synthesis techniques have aroused an interest in the UHTC area. The UHTCs in combination with compositional complexity have been proven to be high-potential candidates for applications involving extreme conditions. The thermodynamics of high entropy ceramics is not yet completely understood; however, many computational predictions and approaches are being performed to understand the behavior of the compositionally complex ceramics. All compositionally complex UHTCs consist of borides, carbides, nitrides, carbonitrides, and silicides. These were usually synthesized either as bulk samples or as powders depending on the used synthesis route. In the case of powders, mechanochemical methods such as ball milling, self-propagation high temperature, molten salt-assisted reductions, boro/carbothermal reductions, and sol-gel were used. To ensure homogenous reactions, usually mechanochemically milled samples were preferred for further process except for molten salt assisted. So far, the only compositions synthesized at room temperature are $(Ta_{0.2}Nb_{0.2}Zr_{0.2}Hf_{0.2}W_{0.2})BCN$, $(Ta_{0.2}Nb_{0.2}Zr_{0.2}Hf_{0.2}Ti_{0.2})BCN$, and $(Ta_{0.2}Nb_{0.2}Zr_{0.2}Ti_{0.2}W_{0.2})BCN$, those were prepared using a ball milling approach. Most of the carbides, nitrides, and silicides were prepared by employing spark plasma sintering as dense monoliths. Sol-gel methods have resulted in obtaining borides, carbides, and nitrides as powders which in turn can be used as prerequisites for spark plasma sintering or hot pressing to obtain dense samples.

In the case of borides, various borides have been synthesized such as mono, di, tetra, hexa, dodeca borides and M_3B_4. These borides were obtained as single-phase compounds during densification. The trend in the properties caused by the anisotropy in the crystal structure suggested to consider the lattice mismatch over atomic size mismatch for the determination of the deviation parameter δ.

In the case of carbides, the reactions were straightforward with carbothermal reductions either as powders or reactive densification. Also, the sintering of mixtures of binary carbides was also performed to obtain a dense sample. The nitrides proved to be a problem due to the intrinsically high

N_2 fugacity of nitrogen. This problem can be overcome by the sol-gel process. Although borides and carbides were also synthesized by using high-pressure high-temperature techniques, due to the air-tight conditions, the above process seems like a viable alternative for the nitrides.

Although significant work has been performed in the field of synthesis of compositionally complex UHTCs, most of the literature can be found on borides and carbides, with less focus on nitrides and silicides. The mechanical properties such as elastic moduli, density, and hardness were measured, but the other properties such as fracture toughness and high-temperature properties are yet to be investigated.

Acknowledgments

DTT gratefully acknowledges funding from the German Academic Exchange Service (Deutscher Akademischer Austauschdienst, DAAD) in the form of a doctoral fellowship grant. The authors acknowledge furthermore funding from DAAD within the frame of the Programs for Project-Related Personal Exchange (PPP, project no. 57601381, “Compositionally Complex Metal Carbides and Carbonitrides”). Also, SAK and EI received funding from the German Research Foundation (Deutsche Forschungsgemeinschaft, DFG) within the Research Training Group RTG 2561 (project no. 413956820, “Materials Compounds from Composite Materials”).

5. References

[1] H. Chen, H. Xiang, F.Z. Dai, J. Liu, Y. Zhou, Porous high entropy (Zr0.2Hf0.2Ti0.2Nb0.2Ta0.2)B2: A novel strategy towards making ultrahigh temperature ceramics thermal insulating, *J. Mater. Sci. Technol. 35* (2019) 2404–2408. https://doi.org/10.1016/j.jmst.2019.05.059.

[2] M. Qin, Q. Yan, H. Wang, C. Hu, K.S. Vecchio, J. Luo, High-entropy monoborides: Towards super hard materials, *Scr. Mater. 189* (2020) 101–105. https://doi.org/10.1016/j.scriptamat.2020.08.018.

[3] Y. Zhang, Z. Bin Jiang, S.K. Sun, W.M. Guo, Q.S. Chen, J.X. Qiu, K. Plucknett, H.T. Lin, Microstructure and mechanical properties of high-entropy borides derived from boro/carbothermal reduction, *J. Eur. Ceram. Soc. 39* (2019) 3920–3924. https://doi.org/10.1016/j.jeurceramsoc.2019.05.017.

[4] Z.Q. Linjing Qiao, Yi Liu, Yu Gao, Jianqiang Bi, Yonghan Li, Chen Liu, Jian Gao, Weili Wang, First-principles prediction, fabrication and characterization of (Hf0.2Nb0.2Ta0.2Ti0.2Zr0.2)B2 high-entropy borides, *Ceram. Int. 48* (2022) 17234–17245. https://doi.org/10.1016/j.ceramint.2022.02.281.

[5] F. Monteverde, F. Saraga, M. Gaboardi, J.R. Plaisier, Compositional pathways and anisotropic thermal expansion of high-entropy transition metal diborides, *J. Eur. Ceram. Soc. 41* (2021) 6255–6266. https://doi.org/10.1016/j.jeurceramsoc.2021.05.053.

[6] M. Li, X. Zhao, G. Shao, H. Wang, J. Zhu, W. Liu, B. Fan, H. Xu, H. Lu, Y. Zhou, R. Zhang, Oscillatory pressure sintering of high entropy (Zr0.2Ta0.2Nb0.2Hf0.2Mo0.2)B2 ceramic, *Ceram. Int. 47* (2021) 8707–8710. https://doi.org/10.1016/j.ceramint.2020.11.108.

[7] G. Tallarita, R. Licheri, S. Garroni, R. Orrù, G. Cao, Novel processing route for the fabrication of bulk high-entropy metal diborides, *Scr. Mater. 158* (2019) 100–104. https://doi.org/10.1016/j.scriptamat.2018.08.039.

[8] M. Qin, Q. Yan, Y. Liu, H. Wang, C. Wang, T. Lei, K.S. Vecchio, H.L. Xin, T.J. Rupert, J. Luo, Bulk high-entropy hexaborides, *J. Eur. Ceram. Soc. 41* (2021) 5775–5781. https://doi.org/10.1016/j.jeurceramsoc.2021.05.027.

[9] L. Qiao, Y. Liu, Y. Gao, J. Bi, Y. Li, C. Liu, J. Gao, W. Wang, Z. Qian, First-principles prediction, fabrication and characterization of (Hf0.2Nb0.2Ta0.2Ti0.2Zr0.2)B2 high-entropy borides, *Ceram. Int. 48* (2022) 17234–17245. https://doi.org/10.1016/j.ceramint.2022.02.281.

[10] Y. Yang, J. Bi, K. Sun, L. Qiao, Y. Liu, Y. Li, H. Wang, Y. Liang, M. Shang, Novel (Hf0.2Zr0.2Ta0.2V0.2Nb0.2)B2 high entropy diborides with superb hardness sintered by SPS under a mild condition, *Ceram. Int. 48* (2022) 30859–30867. https://doi.org/10.1016/j.ceramint.2022.07.040.

[11] X.F. Wei, J.X. Liu, F. Li, Y. Qin, Y.C. Liang, G.J. Zhang, High entropy carbide ceramics from different starting materials, *J. Eur. Ceram. Soc. 39* (2019) 2989–2994. https://doi.org/10.1016/j.jeurceramsoc.2019.04.006.

[12] Y. Zhang, W.M. Guo, Z. Bin Jiang, Q.Q. Zhu, S.K. Sun, Y. You, K. Plucknett, H.T. Lin, Dense high-entropy boride ceramics with ultra-high hardness, *Scr. Mater. 164* (2019) 135–139. https://doi.org/10.1016/j.scriptamat.2019.01.021.

[13] F. Wang, X. Yan, T. Wang, Y. Wu, L. Shao, M. Nastasi, Y. Lu, B. Cui, Irradiation damage in (Zr0.25Ta0.25Nb0.25Ti0.25)C high-entropy carbide ceramics, *Acta Mater. 195* (2020) 739–749. https://doi.org/10.1016/j.actamat.2020.06.011.

[14] S. Guan, H. Liang, Q. Wang, L. Tan, F. Peng, Synthesis and Phase Stability of the High-Entropy Carbide (Ti0.2Zr0.2Nb0.2Ta0.2Mo0.2)C under Extreme Conditions, *Inorg. Chem. 60* (2021) 3807–3813. https://doi.org/10.1021/acs.inorgchem.0c03319.

[15] E.W. Neuman, G.E. Hilmas, W.G. Fahrenholtz, Transition metal diboride-silicon carbide-boron carbide ceramics with super-high hardness and strength, *J. Eur. Ceram. Soc. 42* (2022) 6795–6801. https://doi.org/10.1016/j.jeurceramsoc.2022.08.019.

[16] O.F. Dippo, N. Mesgarzadeh, T.J. Harrington, G.D. Schrader, K.S. Vecchio, Bulk high-entropy nitrides and carbonitrides, *Sci. Rep. 10* (2020) 21288. https://doi.org/10.1038/s41598-020-78175-8.

[17] Y.C. Lin, S.Y. Hsu, Y.T. Lai, P.H. Kuo, S.Y. Tsai, J.G. Duh, Effect of the N2/(Ar+N2) ratio

on mechanical properties of high entropy nitride (Cr0.35Al0.25Nb0.12Si0.08V0.20)Nx films, *Mater. Chem.* Phys. *274* (2021) 125195. https://doi.org/10.1016/j.matchemphys.2021.125195.

[18] J. Guan, D. Li, Z. Yang, B. Wang, D. Cai, X. Duan, P. He, D. Jia, Y. Zhou, Synthesis and thermal stability of novel high-entropy metal boron carbonitride ceramic powders, *Ceram. Int. 46* (2020) 26581–26589. https://doi.org/10.1016/j.ceramint.2020.07.126.

[19] W. Zhang, L. Chen, C. Xu, W. Lu, Y. Wang, J. Ouyang, Y. Zhou, Densification, microstructure and mechanical properties of multicomponent (TiZrHfNbTaMo)C ceramic prepared by pressureless sintering, *J. Mater. Sci. Technol. 72* (2021) 23–28. https://doi.org/10.1016/j.jmst.2020.07.019.

[20] Z. Peng, W. Sun, X. Xiong, H. Zhang, F. Guo, J. Li, Novel refractory high-entropy ceramics: Transition metal carbonitrides with superior ablation resistance, *Corros. Sci. 184* (2021) 109359. https://doi.org/10.1016/j.corsci.2021.109359.

[21] B. Ye, T. Wen, D. Liu, Y. Chu, Oxidation behavior of (Hf 0.2 Zr 0.2 Ta 0.2 Nb 0.2 Ti 0.2)C high-entropy ceramics at 1073-1473 K in air, *Corros. Sci. 153* (2019) 327–332. https://doi.org/10.1016/j.corsci.2019.04.001.

[22] E. Ionescu, S. Bernard, R. Lucas, P. Kroll, S. Ushakov, A. Navrotsky, R. Riedel, Polymer-Derived Ultra-High Temperature Ceramics (UHTCs) and Related Materials, *Adv. Eng. Mater. 21* (2019) 1–24. https://doi.org/10.1002/adem.201900269.

[23] P. Šolcová, M. Nižňanský, J. Schulz, P. Brázda, P. Ecorchard, M. Vilémová, V. Tyrpekl, Preparation of High-Entropy (Ti, Zr, Hf, Ta, Nb) Carbide Powder via Solution Chemistry, *Inorg. Chem. 60* (2021) 7617–7621. https://doi.org/10.1021/acs.inorgchem.1c00776.

[24] Q. Zhao, J. Mei, W. Jin, Q. Jiang, A novel approach to the rapid synthesis of high-entropy carbide nanoparticles, *J. Am. Ceram. Soc. 103* (2020) 4733–4737. https://doi.org/10.1111/jace.17173.

[25] R. Adalati, M. Sharma, S. Sharma, A. Kumar, G. Malik, R. Boukherroub, R. Chandra, Metal nitrides as efficient electrode material for supercapacitors*: A review, J. Energy Storage. 56* (2022) 105912. https://doi.org/10.1016/j.est.2022.105912.

[26] E. Chicardi, C. García-Garrido, J. Hernández-Saz, F.J. Gotor, Synthesis of all equiatomic five-transition metals High Entropy Carbides of the IVB (Ti, Zr, Hf) and VB (V, Nb, Ta) groups by a low-temperature route, *Ceram. Int. 46* (2020) 21421–21430. https://doi.org/10.1016/j.ceramint.2020.05.240.

[27] T. Stasiak, P. Souček, V. Buršíková, N. Koutná, Z. Czigány, K. Balázsi, P. Vašina, Synthesis and characterization of the ceramic refractory metal high entropy nitride thin films from Cr-Hf-Mo-Ta-W system, *Surf. Coatings Technol. 449* (2022). https://doi.org/10.1016/j.surfcoat.2022.128987.

[28] T.H. Hsieh, C.H. Hsu, C.Y. Wu, J.Y. Kao, C.Y. Hsu, Effects of deposition parameters on the structure and mechanical properties of high-entropy alloy nitride films, *Curr. Appl. Phys. 18* (2018) 512–518. https://doi.org/10.1016/j.cap.2018.02.015.

[29] T. Jin, X. Sang, R.R. Unocic, R.T. Kinch, X. Liu, J. Hu, H. Liu, S. Dai, Mechanochemical-Assisted Synthesis of High-Entropy Metal Nitride via a Soft Urea Strategy, *Adv. Mater. 30* (2018) 1–5. https://doi.org/10.1002/adma.201707512.

[30] P. Sarker, T. Harrington, C. Toher, C. Oses, M. Samiee, J.P. Maria, D.W. Brenner, K.S. Vecchio, S. Curtarolo, High-entropy high-hardness metal carbides discovered by entropy descriptors, *Nat. Commun. 9* (2018) 1–10. https://doi.org/10.1038/s41467-018-07160-7.

[31] F. Li, Y. Lu, X.G. Wang, W. Bao, J.X. Liu, F. Xu, G.J. Zhang, Liquid precursor-derived high-entropy carbide nanopowders, *Ceram. Int. 45* (2019) 22437–22441. https://doi.org/10.1016/j.ceramint.2019.07.244.

[32] S.Y. Hsu, Y.T. Lai, S.Y. Chang, S.Y. Tsai, J.G. Duh, Combinatorial synthesis of reactively co-sputtered high entropy nitride (HfNbTiVZr)N coatings: Microstructure and mechanical properties, *Surf. Coatings Technol. 442* (2022) 128564. https://doi.org/10.1016/j.surfcoat.2022.128564.

[33] A. V. Pshyk, A. Vasylenko, B. Bakhit, L. Hultman, P. Schweizer, T.E.J. Edwards, J. Michler, G. Greczynski, High-entropy transition metal nitride thin films alloyed with Al: Microstructure, phase composition and mechanical properties, *Mater. Des. 219* (2022) 110798. https://doi.org/10.1016/j.matdes.2022.110798.

[34] J. Gild, J. Braun, K. Kaufmann, E. Marin, T. Harrington, P. Hopkins, K. Vecchio, J. Luo, A high-entropy silicide: (Mo0.2Nb0.2Ta0.2Ti0.2W0.2)Si2, *J. Mater. 5* (2019) 337–343. https://doi.org/10.1016/j.jmat.2019.03.002.

[35] L. Feng, W.G. Fahrenholtz, G.E. Hilmas, Y. Zhou, Synthesis of single-phase high-entropy carbide powders, *Scr. Mater. 162* (2019) 90–93. https://doi.org/10.1016/j.scriptamat.2018.10.049.

[36] K. Wang, L. Chen, C. Xu, W. Zhang, Z. Liu, Y. Wang, J. Ouyang, X. Zhang, Y. Fu, Y. Zhou, Microstructure and mechanical properties of (TiZrNbTaMo)C high-entropy ceramic, *J. Mater. Sci. Technol. 39* (2020) 99–105. https://doi.org/10.1016/j.jmst.2019.07.056.

[37] Y. Wu, J. Xiong, Z. Guo, M. Yang, J. Chen, S. Xiong, H. Fan, J. Luo, Microstructure and fracture toughness of Ti (C 0 . 7 N 0 . 3) -WC-Ni cermets, *Int. Journal of Refractory Metals and Hard Materials. 29* (2011) 85–89. http://dx.doi.org/10.1016/j.ijrmhm.2010.08.004.

[38] Z. Anwer, S. Huang, J. Vleugels, Liquid phase assisted synthesis of (Ti, V, Nb, Ta, W)C-Ni high entropy carbide cermets by conventional pressureless sintering, *Int. J. Refract. Met. Hard Mater. 107* (2022) 105914. https://doi.org/10.1016/j.ijrmhm.2022.105914.

[39] J. Song, G. Chen, H. Xiang, F. Dai, S. Dong, W. Han, X. Zhang, Y. Zhou, Regulating the formation ability and mechanical properties of high-entropy transition metal carbides by carbon stoichiometry, *J. Mater. Sci. Technol. 121* (2022) 181 189.https://doi.org/10.1016/j.jmst.2021.12.063.

[40] E. Chicardi, C. García-Garrido, F.J. Gotor, Low temperature synthesis of an equiatomic (TiZrHfVNb)C5 high entropy carbide by a mechanically-induced carbon diffusion route, *Ceram. Int. 45* (2019) 21858–21863. https://doi.org/10.1016/j.ceramint.2019.07.195.

[41] T.J. Harrington, J. Gild, P. Sarker, C. Toher, C.M. Rost, O.F. Dippo, C. McElfresh, K.Kaufmann, E. Marin, L. Borowski, P.E. Hopkins, J. Luo, S. Curtarolo, D.W. Brenner, K.S. Vecchio, Phase stability and mechanical properties of novel high entropy transition metal carbides, *Acta Mater. 166* (2019) 271–280. https://doi.org/10.1016/j.actamat.2018.12.054.

[42] J. Zhou, J. Zhang, F. Zhang, B. Niu, L. Lei, W. Wang, High-entropy carbide*:* A novel class of multicomponent ceramics, *Ceram. Int. 44* (2018) 22014–22018. https://doi.org/10.1016/j.ceramint.2018.08.100.

[43] H.R. Mao, E.T. Dong, S.B. Jin, X.M. Qiu, P. Shen, Ultrafast high-temperature synthesis and densification of high-entropy carbides, *J. Eur. Ceram. Soc. 42* (2022) 4053–4065.https://doi.org/10.1016/J.JEURCERAMSOC.2022.03.054.

[44] E. Castle, T. Csanádi, S. Grasso, J. Dusza, M. Reece, Processing and Properties of High-Entropy Ultra-High Temperature Carbides, *Sci. Rep. 8* (2018) 1–12. https://doi.org/10.1038/s41598-018-26827-1.

[45] D. Liu, Y. Hou, A. Zhang, J. Han, J. Zhang, J. Meng, H. Su, Experimental studies on critical compositions for fabricating single-phase high entropy carbides based on the calculated phase diagram of (VNbTaMoW)0.5Cx (0 < x < 0.6), *J. Eur. Ceram. Soc. 41* (2021) 7488–7497. https://doi.org/10.1016/j.jeurceramsoc.2021.08.037.

[46] Y. Wang, B. Zhang, C. Zhang, J. Yin, M.J. Reece, Ablation behaviour of (Hf-Ta-Zr-Nb)C high entropy carbide ceramic at temperatures above 2,100 °C, *J. Mater. Sci. Technol. 113* (2022) 40–47. https://doi.org/10.1016/j.jmst.2021.09.064.

[47] J. Dusza, P. Švec, V. Girman, R. Sedlák, E.G. Castle, T. Csanádi, A. Kovalčíková, M.J.Reece, Microstructure of (Hf-Ta-Zr-Nb)C high-entropy carbide at micro and nano/atomic level, *J.Eur. Ceram. Soc. 38* (2018) 4303–4307. https://doi.org/10.1016/j.jeurceramsoc.2018.05.006.

[48] C. Zhang, X. Lu, C. Wang, X. Sui, Y. Wang, H. Zhou, J. Hao, Tailoring the microstructure, mechanical and tribocorrosion performance of (CrNbTiAlV)Nx high-entropy nitride films by controlling nitrogen flow, *J. Mater. Sci. Technol. 107* (2022) 172–182.https://doi.org/10.1016/j.jmst.2021.08.032.

[49] J. Li, Y. Chen, Y. Zhao, X. Shi, S. wang, S. Zhang, Super-hard (MoSiTiVZr)Nx high-entropy nitride coatings, *J. Alloys Compd. 926 (2022) 166807*. https://doi.org/10.1016/j.jallcom.2022.166807.

[50] D. Moskovskikh, S. Vorotilo, V. Buinevich, A. Sedegov, K. Kuskov, A. Khort, C. Shuck, M. Zhukovskyi, A. Mukasyan, Extremely hard and tough high entropy nitride ceramics, *Sci. Rep.*

10 (2020) 19874. https://doi.org/10.1038/s41598-020-76945-y.

[51] A. Kretschmer, D. Holec, K. Yalamanchili, H. Rudigier, M. Hans, J.M. Schneider, P.H. Mayrhofer, Strain-stabilized Al-containing high-entropy sublattice nitrides, *Acta Mater. 224*(2022) 117483. https://doi.org/10.1016/j.actamat.2021.117483.

[52] H. Liu, B. Du, Y. Chu, Synthesis of the ternary metal carbide solid-solution ceramics by polymer-derived-ceramic route, *J. Am. Ceram. Soc. 103* (2020) 2970–2974. https://doi.org/10.1111/jace.16993.

[53] A.L. Tomas-Garcia, Q. Li, J.O. Jensen, N.J. Bjerrum, High surface area tungsten carbides: Synthesis, characterization and catalytic activity towards the hydrogen evolution reaction in phosphoric acid at elevated temperatures, *Int. J. Electrochem. Sci. 9* (2014) 1016–1032.

[54] D. Liu, A. Zhang, J. Jia, J. Meng, B. Su, Phase evolution and properties of (VNbTaMoW)C high entropy carbide prepared by reaction synthesis, *J. Eur. Ceram. Soc. 40* (2020) 2746–2751. https://doi.org/10.1016/j.jeurceramsoc.2020.03.020.

[55] A. Sedegov, S. Vorotilo, V. Tsybulin, K. Kuskov, D. Moscovskikh, Synthesis and study of high-entropy ceramics based on the carbides of refractory metals, *IOP Conf. Ser. Mater. Sci. Eng. 558* (2019). https://doi.org/10.1088/1757-899X/558/1/012043.

[56] B. Du, H. Liu, Y. Chu, Fabrication and characterization of polymer-derived high-entropy carbide ceramic powders, *J. Am. Ceram. Soc. 103* (2020) 4063–4068.https://doi.org/10.1111/jace.17134.

[57] Liu, H. L., Feng-Zhen, D. A. N. G., De-Wei, N. I., Chang-Qing, L. I. U., Yun-Long, X. U. E.,& Yuan-Ting, W. U, Preparation of Single-phase High Entropy Carbides by a Modified Citric Acid Complexing Method (2021).

[58] F. William G, G.E. Hilmas, Ultra-High Temperature Ceramics: Materials for Extreme Environments Department of Materials Science and Engineering Missouri University of Science and Technology, Rolla, MO 65049, *Scr. Mater. 129* (2017) 94–99. https://doi.org/10.1016/j.scriptamat.2016.10.018.

[59] P. Zhao, J. Zhu, M. Li, G. Shao, H. Lu, H. Wang, J. He, Theoretical and experimental investigations on the phase stability and fabrication of high-entropy monoborides, *J. Eur. Ceram. Soc. 43* (2023) 2320–2330. https://doi.org/10.1016/j.jeurceramsoc.2023.01.026.

[60] P. Zhao, J. Zhu, Y. Zhang, G. Shao, H. Wang, M. Li, W. Liu, B. Fan, H. Xu, H. Lu, Y. Zhou, R. Zhang, A novel high-entropy monoboride (Mo0.2Ta0.2Ni0.2Cr0.2W0.2)B with super hardness and low thermal conductivity, *Ceram. Int. 46* (2020) 26626–26631. https://doi.org/10.1016/j.ceramint.2020.07.131.

[61] A. Salian, P. Sengupta, I. Vishalakshi Aswath, A. Gowda, S. Mandal, A review on high entropy silicides and silicates: Fundamental aspects, synthesis, properties, *Int. J. Appl. Ceram. Technol. 20* (2023) 2635–2660. https://doi.org/10.1111/ijac.14422.

[62] A.Y. Pak, P.S. Grinchuk, A.A. Gumovskaya, Y.Z. Vassilyeva, Synthesis of transition metal carbides and high-entropy carbide TiZrNbHfTaC5 in self-shielding DC arc discharge plasma, *Ceram. Int. 48* (2022) 3818–3825. https://doi.org/10.1016/j.ceramint.2021.10.165.

[63] Y. Yang, J. Bi, X. Gao, K. Sun, L. Qiao, G. Liang, H. Wang, Facile synthesis of nanocrystalline high-entropy diboride powders by a simple sol-gel method and their performance in supercapacitor, *Ceram. Int. 49* (2023) 19523–19527. https://doi.org/10.1016/j.ceramint.2023.02.170.

[64] Y.C. Shanshan Ning, Tongqi Wen, Beilin Ye, Low-temperature molten salt synthesis of high-entropy carbide, *J. Am. Ceram. Soc. 103* (2019) 2244–2251. https://doi.org/https://doi.org/10.1111/jace.16896.

[65] S. Ye, J. Zhu, P. Li, M. Li, N. Yan, H. Wang, Study on microstructure, mechanical properties and thermal performance of single-phase (Ti, Zr, Hf)B2 solid solution, *Mater. Today Commun. 34* (2023) 105228. https://doi.org/10.1016/j.mtcomm.2022.105228.

[66] D. Yu, J. Yin, B. Zhang, X. Liu, Z. Huang, Recent development of high-entropy transitional carbides: A review, *J. Ceram. Soc. Japan. 128* (2020) 329–335. https://doi.org/10.2109/jcersj2.19242.

[67] B. Li, C. Liu, Z. Fang, Z. Yang, F. Ding, L. Bai, C. Wang, F. Yuan, Synthesis of single-phase (ZrTiTaNbMo)C high-entropy carbide powders via magnesiothermic reduction process, *J. Eur. Ceram. Soc. 42* (2022) 6767–6773. https://doi.org/10.1016/j.jeurceramsoc.2022.08.025.

[68] Y. Qin, J.X. Liu, F. Li, X. Wei, H. Wu, G.J. Zhang, A high entropy silicide by reactive spark plasma sintering, *J. Adv. Ceram. 8* (2019) 148–152. https://doi.org/10.1007/s40145-019-0319-3.

[69] J. Xing, P. Foroughi, S. Mondal, S. Sun, Z. Cheng, Facile and economical routes toward novel high-entropy metal nitride high-temperature ceramic nanograin powders, *MRS Commun. 12* (2022) 183–187. https://doi.org/10.1557/s43579-022-00159-8.

[70] M. Qin, Q. Yan, H. Wang, C. Hu, K.S. Vecchio, J. Luo, High-entropy monoborides: Towards superhard materials, *Scr. Mater. 189* (2020) 101–105. https://doi.org/10.1016/j.scriptamat.2020.08.018.

[71] M. Qin, Q. Yan, Y. Liu, J. Luo, A new class of high-entropy M3B4 borides, *J. Adv. Ceram. 10* (2021) 166–172. https://doi.org/10.1007/s40145-020-0438-x.

[72] M. Qin, Q. Yan, H. Wang, K.S. Vecchio, J. Luo, High-entropy rare earth tetraborides, *J. Eur. Ceram. Soc. 41* (2021) 2968–2973. https://doi.org/10.1016/j.jeurceramsoc.2020.12.019.

[73] J. Liu, Q.Q. Yang, J. Zou, W.M. Wang, X.G. Wang, Z.Y. Fu, Strong high-entropy diboride ceramics with oxide impurities at 1800°C, *Sci. China Mater. 66* (2023) 2061–2070. https://doi.org/10.1007/s40843-022-2287-7.

[74] M. Qin, J. Gild, H. Wang, T. Harrington, K.S. Vecchio, J. Luo, Dissolving and stabilizing soft WB2 and MoB2 phases into high-entropy borides via boron-metals reactive sintering to attain higher hardness, *J. Eur. Ceram. Soc. 40* (2020) 4348–4353. https://doi.org/10.1016/j.jeurceramsoc.2020.03.063.

[75] S. Kavak, K.G. Bayrak, M. Mansoor, M. Kaba, E. Ayas, Ö. Balcı-Çağıran, B. Derin, M.L. Öveçoğlu, D. Ağaoğulları, First principles calculations and synthesis of multi-phase (HfTiWZr)B2 high entropy diboride ceramics: Microstructural, mechanical and thermal characterization, *J. Eur. Ceram. Soc. 43* (2023) 768–782. https://doi.org/10.1016/j.jeurceramsoc.2022.10.047.

[76] Z.J. Huang, L.F. Su, L. Xu, Y.Z. Zhou, W.M. Guo, H.T. Lin, Dense (Hf0.2Mo0.2Ta0.2Nb0.2Ti0.2)B2 ceramics prepared by pressureless sintering with Ni additives, *Ceram. Int. 49* (2023) 27651–27656. https://doi.org/10.1016/j.ceramint.2023.05.192.

[77] J. Gild, Y. Zhang, T. Harrington, S. Jiang, T. Hu, M.C. Quinn, W.M. Mellor, N. Zhou, K. Vecchio, J. Luo, High-Entropy Metal Diborides: A New Class of High-Entropy Materials and a New Type of Ultrahigh Temperature Ceramics, *Sci. Rep. 6* (2016) 37946. https://doi.org/10.1038/srep37946.

[78] Y. Wang, Processing and properties of high entropy carbides, *Adv. Appl. Ceram. 121* (2022) 57–78. https://doi.org/10.1080/17436753.2021.2014277.

[79] B.R. Golla, A. Mukhopadhyay, B. Basu, S.K. Thimmappa, Review on ultra-high temperature boride ceramics, *Prog. Mater. Sci. 111* (2020) 100651. https://doi.org/10.1016/j.pmatsci.2020.100651.

[80] B. Ye, T. Wen, M.C. Nguyen, L. Hao, C.Z. Wang, Y. Chu, First-principles study, fabrication and characterization of (Zr 0.25 Nb 0.25 Ti 0.25 V 0.25)C high-entropy ceramics, *Acta Mater. 170* (2019) 15–23. https://doi.org/10.1016/j.actamat.2019.03.021.

[81] H. Xiang, Y. Xing, F. Zhi Dai, H. Wang, L. Su, L. Miao, G. Zhang, Y. Wang, X. Qi, L. Yao, H. Wang, B. Zhao, J. Li, Y. Zhou, High-entropy ceramics: Present status, challenges, and a look forward, *J Adv Ceram 10*, 385–441 2021. https://doi.org/10.1007/s40145-021-0477-y.

[82] J. Liu, X. Shen, Y. Wu, F. Li, Y. Liang, G. Zhang, Mechanical properties of hot-pressed high-entropy diboride-based ceramics, *J. Adv. Ceram. 9* (2020) 503–510. https://doi.org/https://doi.org/10.1007/s40145-020-0383-8.

[83] J. Billingham, P.S. Bell, M.H. Lewis, Vacancy short-range order in substoichiometric transition metal carbides and nitrides with the NaCl structure. I. Electron diffraction studies of short-range ordered compounds, *Acta Crystallogr. Sect. A. 28* (1972) 602–606. https://doi.org/10.1107/S0567739472001524.

[84] X.X. Yu, G.B. Thompson, C.R. Weinberger, Influence of carbon vacancy formation on the elastic constants and hardening mechanisms in transition metal carbides, *J. Eur. Ceram. Soc. 35* (2015) 95–103. https://doi.org/10.1016/j.jeurceramsoc.2014.08.021.

[85] Beilin Ye, Shanshan Ning, Da Liu, Tongqi Wen, One-step synthesis of coral-like high-entropy metal carbide powders, *J. Am. Ceram. Soc. 102* (2019) 6372–6378.

https://doi.org/https://doi.org/10.1111/jace.16514.
[86] D. Demirskyi, T. Nishimura, T.S. Suzuki, Y. Sakka, O. Vasylkiv, K. Yoshimi, High-temperature toughening in ternary medium-entropy (Ta1/3Ti1/3Zr1/3)C carbide consolidated using spark-plasma sintering, *J. Asian Ceram. Soc. 8* (2020) 1262–1270. https://doi.org/10.1080/21870764.2020.1840703.
[87] S. Shivakumar, M. Qin, D. Zhang, C. Hu, Q. Yan, J. Luo, A new type of compositionally complex M5Si3 silicides: Cation ordering and unexpected phase stability, *Scr. Mater. 212* (2022) 114557. https://doi.org/10.1016/j.scriptamat.2022.114557.
[88] H. Liu, S. Ning, Fabrication of High-Entropy Disilicide Nanopowders via Molten Salt-Assisted Magnesium Thermal Reduction, *Res. Sq. Rapid Commun.* (2020) 1–9.
[89] Beilin Ye, Che Fan, Yangjie Han, Mengdong Ma, Synthesis of high-entropy diboride nanopowders via molten salt-mediated magnesiothermic reduction, *J. Am. Ceram. Soc. 103* (2020) 4738–4741. https://doi.org/https://doi.org/10.1111/jace.17184.
[90] W. Zhang, F. Guo, R. Zhang, D. Liu, X. Wang, X. Zhao, A simple route to synthesize high-entropy carbide (Hf0.2Zr0.2Ti0.2Ce0.2La0.2)C1-δ nanoparticles with large covalent radius difference, *Ceram. Int. 49* (2023) 38566–38574. https://doi.org/10.1016/j.ceramint.2023.09.189.
[91] Z. Zhang, S. Zhu, Y. Liu, L. Liu, Z. Ma, Phase structure, mechanical properties and thermal properties of high-entropy diboride (Hf0.25Zr0.25Ta0.25Sc0.25)B2, *J. Eur. Ceram. Soc. 42* (2022) 5303–5313. https://doi.org/10.1016/j.jeurceramsoc.2022.05.066.
[92] S. Failla, P. Galizia, S. Fu, S. Grasso, D. Sciti, Formation of high entropy metal diborides using arc-melting and combinatorial approach to study quinary and quaternary solid solutions, *J. Eur. Ceram. Soc. 40* (2020) 588–593. https://doi.org/10.1016/j.jeurceramsoc.2019.10.051.
[93] M. Xia, N. Lu, Y. Chen, B. Shen, X. Liang, Microstructures and mechanical properties of (Nb0.25Mo0.25Ta0.25W0.25)C and (Nb0.2Mo0.2Ta0.2W0.2Hf0.2)C high-entropy carbide ceramics produced by arc melting, *Int. J. Refract. Met. Hard Mater. 107* (2022) 105859. https://doi.org/10.1016/j.ijrmhm.2022.105859.
[94] S. Guan, W. Lin, H. Liang, W. Liang, Y. Tian, D. He, F. Peng, The effect of pressure tuning on the structure and mechanical properties of high-entropy carbides, *Scr. Mater. 216* (2022) 114755. https://doi.org/10.1016/j.scriptamat.2022.114755.
[95] D. Demirskyi, H. Borodianska, T.S. Suzuki, Y. Sakka, K. Yoshimi, O. Vasylkiv, High-temperature flexural strength performance of ternary high-entropy carbide consolidated via spark plasma sintering of TaC, ZrC and NbC, *Scr. Mater. 164* (2019) 12–16. https://doi.org/10.1016/j.scriptamat.2019.01.024.
[96] B. Du, X. Huang, A. Wang, Y. Liu, Y. Cheng, Structure evolutions of the polymer derived medium-/high-entropy metal carbides, *J. Alloys Compd. 939* (2023) 168737. https://doi.org/10.1016/j.jallcom.2023.168737.
[97] S. Iwan, K.C. Burrage, B.C. Storr, S.A. Catledge, Y.K. Vohra, R. Hrubiak, N. Velisavljevic, High-pressure high-temperature synthesis and thermal equation of state of high-entropy transition metal boride, *AIP Adv. 11* (2021). https://doi.org/10.1063/5.0045592.
[98] X. Wang, Y. Zuo, S. Horta, R. He, L. Yang, A. Ostovari Moghaddam, M. Ibáñez, X. Qi, A. Cabot, CoFeNiMnZnB as a High-Entropy Metal Boride to Boost the Oxygen Evolution Reaction, *ACS Appl. Mater. Interfaces. 14* (2022) 48212–48219. https://doi.org/10.1021/acsami.2c11627.
[99] S. Iwan, C.M. Lin, C. Perreault, K. Chakrabarty, C.C. Chen, Y. Vohra, R. Hrubiak, G. Shen, N. Velisavljevic, High-Entropy Borides under Extreme Environment of Pressures and Temperatures, *Materials (Basel). 15* (2022) 1–11. https://doi.org/10.3390/ma15093239.
[100] J. Cui, X. Zheng, W. Bao, J. Liu, F. Xu, G. Zhang, Y. Liang, Coexistence of Super hardness and Metal-Like Electrical Conductivity in High-Entropy Dodecaboride Composite with Atomic-Scale Interlocks, *Nano Lett. 2023 23*(20), 9319–9325. https://doi.org/10.1021/acs.nanolett.3c02506.
[101] X. Zheng, J. Cui, C. Gu, W. Bao, X. Zhou, J. Liu, G. Zhang, W. Zhang, Y. Zhao, S. Wang, Y. Liang, Scripta Materialia Superhard high-entropy dodecaboride with high electrical conductivity, *Scr. Mater. 220* (2022) 114938. https://doi.org/10.1016/j.scriptamat.2022.114938.

[102] P. Zhang, X. Liu, A. Cai, Q. Du, X. Yuan, H. Wang, Y. Wu, S. Jiang, Z. Lu, High-entropy carbide-nitrides with enhanced toughness and sinterability, *Sci. China Mater. 64* (2021) 2037–2044. https://doi.org/10.1007/s40843-020-1610-9.

[103] Z. Wen, H. Meng, S. Jiang, Z. Tang, Y. Liu, Y. Chu, Non-equimolar (Hf, Zr, Ta, W)B2 high entropy diborides enable superior oxidation resistance, *Sci. China Mater. 66* (2023) 3213–3222. https://doi.org/10.1007/s40843-023-2461-y.

[104] W. Zhang, L. Chen, W. Lu, S. Huo, B. Wei, Y. Wang, Y. Zhou, Non-stoichiometry of (TiZrHfVNbTa)Cx and its significance to the microstructure and mechanical properties, *J. Eur. Ceram. Soc. 42* (2022) 6347–6355. https://doi.org/10.1016/j.jeurceramsoc.2022.07.007.

[105] H. Lun, Y. Zeng, X. Xiong, Z. Ye, T. Qian, W. Sun, Y. Wang, Z. Chen, Synthesis of carbide solid solution with multiple components using elemental powder, *Adv. Powder Technol. 31* (2020) 505–509. https://doi.org/10.1016/j.apt.2019.10.019.

[106] F. Wang, F. Monteverde, B. Cui, Will high-entropy carbides and borides be enabling materials for extreme environments?, *Int. J. Extrem. Manuf. 5* (2023). https://doi.org/10.1088/2631-7990/acbd6e.

[107] Q. Xie, X. Liu, Z. Zhang, X. Nian, L. Chen, Investigation of mechanical and electronic properties of a novel quaternary transition-metal nitride Ti0.25W0.25V0.25Ta0.25N, *Mater. Chem. Phys. 310* (2023) 128467. https://doi.org/10.1016/j.matchemphys.2023.128467.

[108] M. Qin, S. Shivakumar, T. Lei, J. Gild, E.C. Hessong, H. Wang, K.S. Vecchio, T.J. Rupert, J. Luo, Processing-dependent stabilization of a dissimilar rare-earth boride in high-entropy (Ti0.2Zr0.2Hf0.2Ta0.2Er0.2)B2 with enhanced hardness and grain boundary segregation, *J. Eur. Ceram. Soc. 42* (2022) 5164–5171. https://doi.org/10.1016/j.jeurceramsoc.2022.05.034.

[109] A.C. Feltrin, F. Akhtar, High-temperature oxidation kinetics of a metastable dual-phase diboride and a high-entropy diboride, *J. Eur. Ceram. Soc. 43* (2023) 7363–7372. https://doi.org/10.1016/j.jeurceramsoc.2023.08.001.

[110] W. Zhang, K. Li, L. Chen, Z. Shi, S. Huo, B. Wei, S.J.L. Kang, Y. Wang, Y. Zhou, The phase decomposition in non-equimolar (ZrHfVNbMoW)Cx complex concentrated carbides via carbon content regulation, *J. Eur. Ceram. Soc. 44* (2023) 1396–1403.https://doi.org/10.1016/j.jeurceramsoc.2023.10.050.

[111] Y. Qin, J.X. Liu, Y. Liang, G.J. Zhang, Equiatomic 9-cation high-entropy carbide ceramics of the IVB, VB, and VIB groups and thermodynamic analysis of the sintering process, *J. Adv. Ceram. 11* (2022) 1082–1092. https://doi.org/10.1007/s40145-022-0594-2.